**Supplementary information for**

# Radical induced disproportionation of alcohols assisted by iodide under acidic conditions

Yang Peng, Yang Huang, Teng Li, Nianxin Rong, Haiwei Jiang, Hexian Shi and Weiran Yang*

*Key Laboratory of Poyang Lake Environment and Resource Utilization (Nanchang University) Ministry of Education, School of Resource, Environmental and Chemical Engineering, Nanchang University, Nanchang 330031, P.R. China*; Email: wyang16@ncu.edu.cn.

## Table of Contents

## 1. Materials

Benzyl alcohol, toluene, benzaldehyde, xylenes, 4-methoxybenzyl alcohol, 4-methylanisole, 4-cyanobenzyl alcohol, 4-tolunitrile, terephthalyl alcohol, para-xylene, terephthalaldehyde, p-tolualdehyde, cinnamic alcohol, cinnamaldehyde, hexane, 57 wt.% hydroiodic acid (HI), 47 wt.% hydrobromic acid (HBr), trifluoro sulfonic acid ($CF_3SO_3H$), trifluoroacetic acid ($CF_3COOH$), lithium iodide(LiI) and 2,5-furandicarbaldehyde (DFF) were purchased from *Shanghai Aladdin Biochemical Technology Co. Ltd.*; 2,5-dimethylfuran and p-anisaldehyde were purchased from *Meryer (Shanghai) Chemical Technology Co., Ltd.*; 2-methyltetrahydrofuran (MTHF), tetrahydrofuran (THF), 5-methyl furfural (5-MF), p-toluic acid and 4-methylphenylene were purchased from *Shanghai Meirel Chemical Technology Co., Ltd.*; toluene and 37 wt.% hydrochloric acid (HCl) were purchased from Xilong Chemical; furan-2,5-diyldimethanol and p-cyanobenzaldehyde were purchased from *Shanghai Adamas Reagent Co., Ltd*; sulfuric acid ($H_2SO_4$) and acetic acid ($CH_3COOH$) were purchased from *Tianjin Damao Chemical Reagent Factory*; potassium iodide (KI) was purchased from *Shanghai Dibai Biotechnology Co., Ltd.*; sodium iodide (NaI) was purchased from *Chinese Medicine Group Chemical Reagent Co. Ltd.*; hypophosphorus acid ($H_3PO_2$) was purchased from *Alfa Aesar Chemical Co., Ltd*. All solvents above not contain BHT. All reagents were used without further purification, and solvents were not distilled unless specified.

## 2. Methods

### Analytical procedures

The product was quantitatively analyzed using an Agilent 7820A gas

chromatograph (GC) manufactured by Agilent, USA. The GC analysis conditions were as follows: chromatographic column HP-5 capillary column (30 m × 320 μm × 0.25 μm); hydrogen flame ionization detector (FID); initial oven temperature was 40 °C, which was first increased at 3 °C $min^{-1}$ to 100 °C, then increased at 10 °C · $min^{-1}$ to 200 °C, and finally maintained for 5 min; injection port temperature was 280 °C; detector temperature was 280 °C; high purity $N_2$ as the carrier gas, flowed at 1.5 mL · $min^{-1}$; split ratio 20:1; the injection volume 1 μL.

The product was qualitatively analyzed using a Thermo Scientific TRACE 1310 GC-MS. GC-MS analysis conditions were as follows: chromatographic column HP-5 capillary column (30 m × 320 μm × 0.25 μm); initial oven temperature was 40 °C, maintained for 5 min; it was first increased at 5 °C · $min^{-1}$ to 100 °C, then increased at 10 °C · $min^{-1}$ to 150 °C, followed by increasing at 20 °C · $min^{-1}$ to 280 °C, and finally maintained for 5 min; ion source temperature was 290 °C; the filament opened at 0 – 2.75 min and 3.4 – 35 min and closed at 2.75 – 3.4 min; with high purity He as the carrier gas, the flow rate of 1.0 ml $min^{-1}$; split ratio 20 : 1; the injection volume 0.2 μL.

**Disproportionation reaction**

A high-pressure stainless-steel reactor, a temperature controller, and IKA magnetic stirring apparatus were supplied by Anhui Kemi Machinery Technology Co., Ltd., China. In a typical reaction, 1.0 mmol HMF, 0.6 mmol NaI, 0.3 mmol $H_2SO_4$, 6 mL THF were sequentially placed into a 50 mL quartz vial. Then, the vial was placed into a 50 mL stainless steel autoclave. And the stainless-steel autoclave was put on the IKA magnetic stirring apparatus. The autoclave was purged by three cycles of pressurization/venting with $N_2$ (300 psi) before being pressurized with $N_2$ (300 psi).

The reaction temperature was set to 180 ℃, heating rate to 9 ℃/min, and heating time to 20 min (Not credited for reaction time). When the reaction was stopped, the reactor was cooled with a water bath. Then, the organic phase was collected for analysis and fractionated to obtain 5-MF and DFF.

**Gram-scale synthesis separation method**

First, the reaction solution was mixed with silica gel and spun dry. Then, the products were separated by silica gel column. Eluent was ethyl acetate: petroleum ether =1:5 mixed solvent. The 5-MF and DFF were separated and then dried by rotary evaporation. Toluene and benzaldehyde were also separated by the similar method. The eluent is ethyl acetate: petroleum ether = 1:100.

**Catalyst detection and analysis**

After the reaction, the product solution was diluted to 10 mL with THF, and 100 uL of the reaction solution was took out and diluted 100 times with water. PH value was measured by PH meter. Starch-KI reagent was used to detect $I_2$ formation. No discoloration proves no $I_2$ formation and vice versa.

**3. Product qualitative and quantitative analysis**

The product was qualitatively analyzed by gas chromatography-mass spectrometry and compared with the standard sample. The product was quantitatively analyzed by external standard method as follows: first, 0.1, 0.3, 0.5, 0.7, 0.9 mmol standard sample was dissolved in 10 mL THF solution to obtain the standard curve of product concentration and peak area. Then the peak area of the sample product is substituted

into the calculation to get the concentration and then calculate the yield.

## 4. Water content of acid

**Table S1** Water content of HI, HBr and HCl.

| Acid | wt.% | Mol. wt. | Density (g/mL) | Volume (uL) | Weight (mg) | Water weight (mg) |
|---|---|---|---|---|---|---|
| HI | 57 | 127.9 | 1.7 | 79 | 134.6 | 57.9 |
| HBr | 47 | 81.0 | 1.5 | 69 | 103.4 | 54.8 |
| HCl | 37 | 37.0 | 1.2 | 50 | 60.0 | 37.8 |
| $H_2SO_4$ | 98 | 98.1 | 1.84 | 33 | 60.1 | 1.2 |

0.6 mmol Acid.

## 5. Comparison of the solubility of NaI in THF and reaction solution.

First, around 0.01ml water was formed during the reaction, thus the NaI solubilities in 6ml THF and 6 ml THF + 0.01ml in 120 ℃ were tested. It can be seen that without the water, 0.6 mmol or higher mount of NaI cannot be completely dissolved in 6 ml THF; but with additional 0.01ml water, even 1.0 mmol NaI can be completely dissolved. Therefore, the small amount of water produced by the reaction can increase the solubility of sodium iodide.

**Table S2** Solubility of NaI in THF and reaction solution.

| NaI (mmol) | NaI (mg) | Temp (℃) | 6 mL THF | 6 mL THF + 0.01 mL $H_2O$ |
|---|---|---|---|---|
| 0.1 | 15 | 120 | ✗ | ✗ |

| | | | | |
|---|---|---|---|---|
| 0.25 | 37.5 | 120 | ⚑ | ⚑ |
| 0.5 | 75 | 120 | ⚑ | ⚑ |
| 0.6 | 90 | 120 | ⚐ | ⚑ |
| 0.8 | 120 | 120 | ⚐ | ⚑ |
| 1.0 | 150 | 120 | ⚐ | ⚑ |

Dissolution: ⚑

Incomplete dissolution: ⚐

## 6. Optimization of reaction parameter

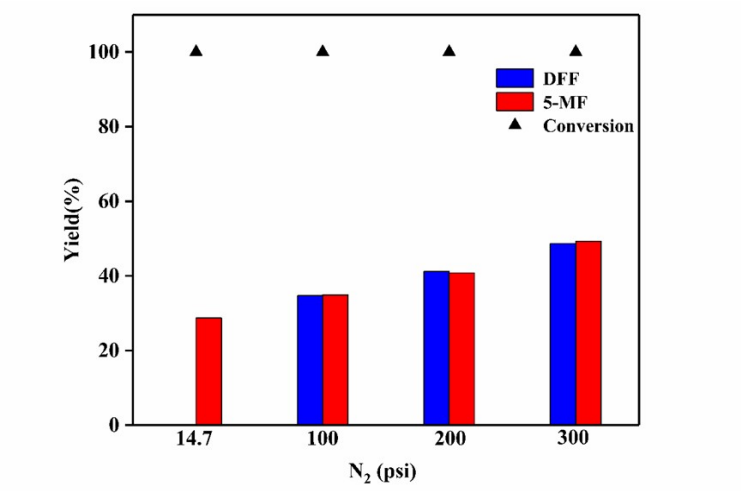


**Figure S1.** Effect of $N_2$ pressure on disproportionation

## 7. The Radical Trapping Experiment

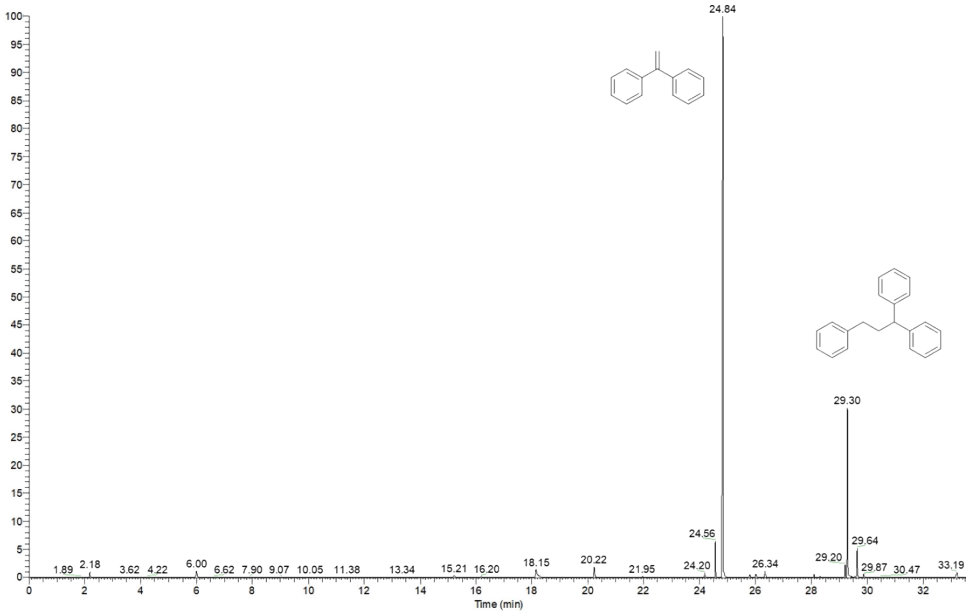


**Figure S2.** $C_{21}H_{20}$ (1,1-diphenylethene captures toluene free radicals) GCMS graph.

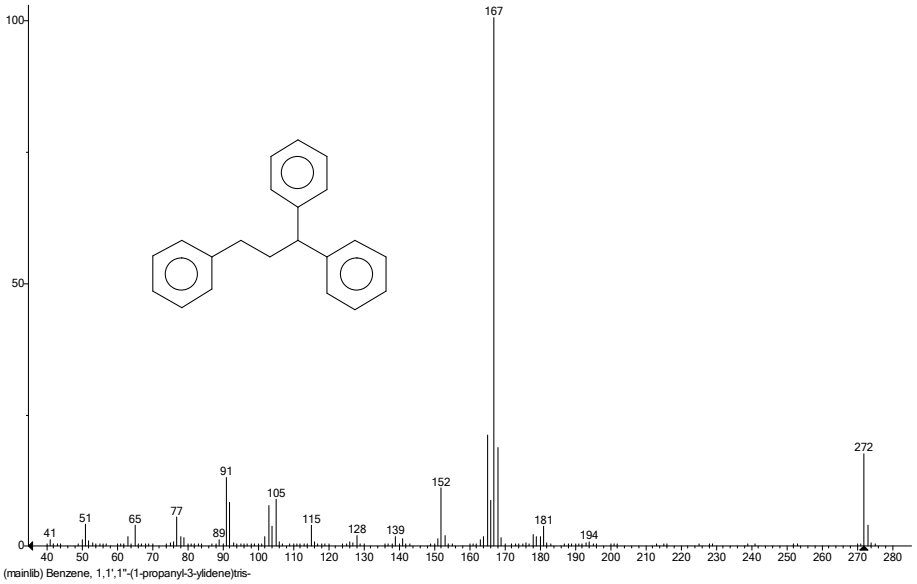


**Figure S3.** $C_{21}H_{20}$ (1,1-diphenylethene captures toluene free radicals) GCMS fragment peak graph.

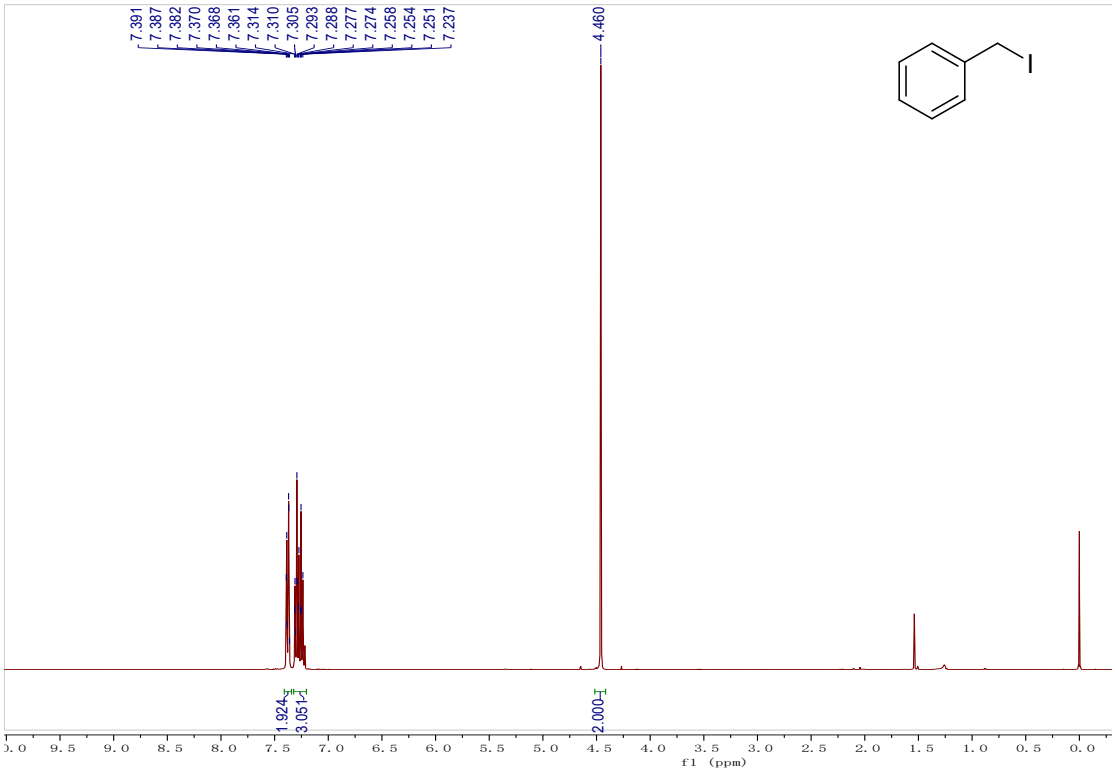


**Figure S4.** $^{1}$HNMR spectrum for compound benzyl iodide. $^{1}$H NMR (400 MHz, $CDCl_3$) δ 7.38 (dt, *J* = 8.3, 2.1 Hz, 2H), 7.33 – 7.21 (m, 3H), 4.46 (s, 2H).

## 8. GC and GCMS data

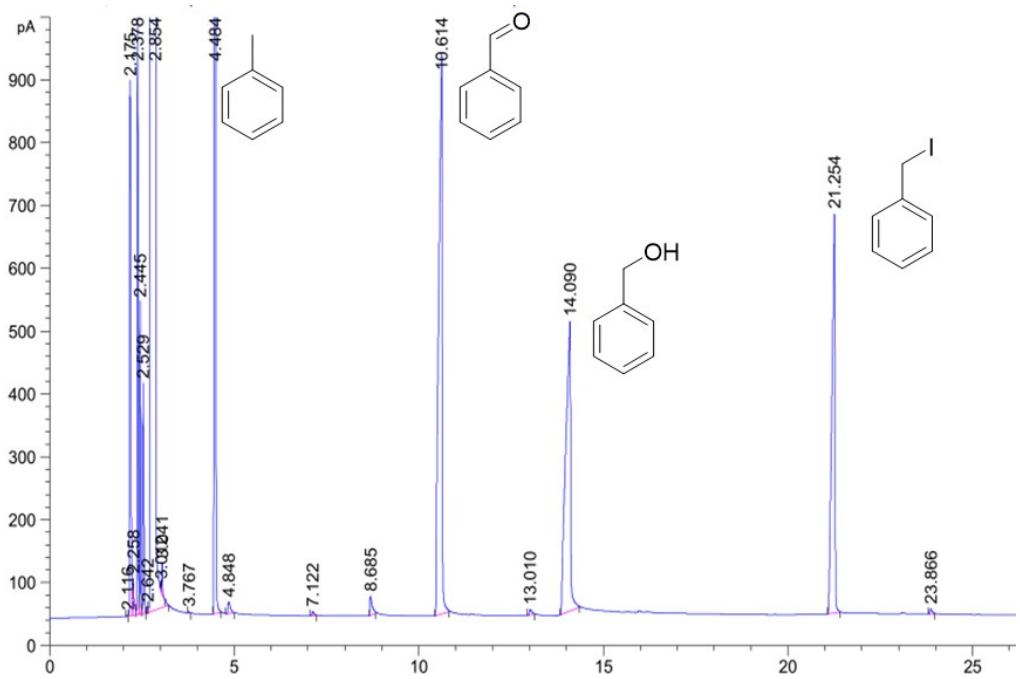

**Figure S5.** GC picture of the reaction between benzyl iodide and benzyl alcohol.

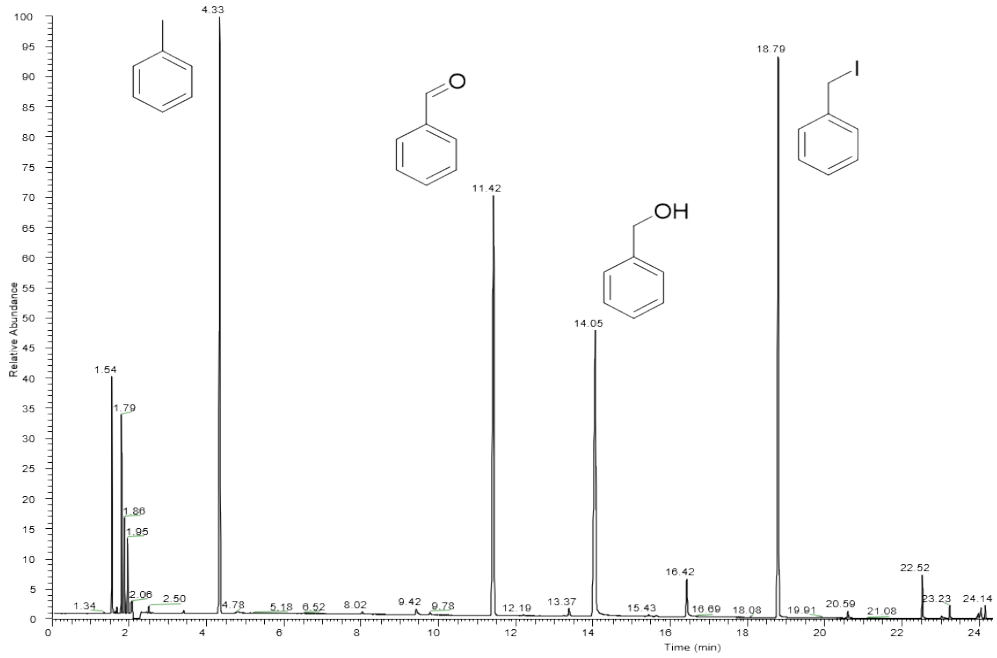


**Figure S6.** GCMS picture of the reaction between benzyl iodide and benzyl alcohol.

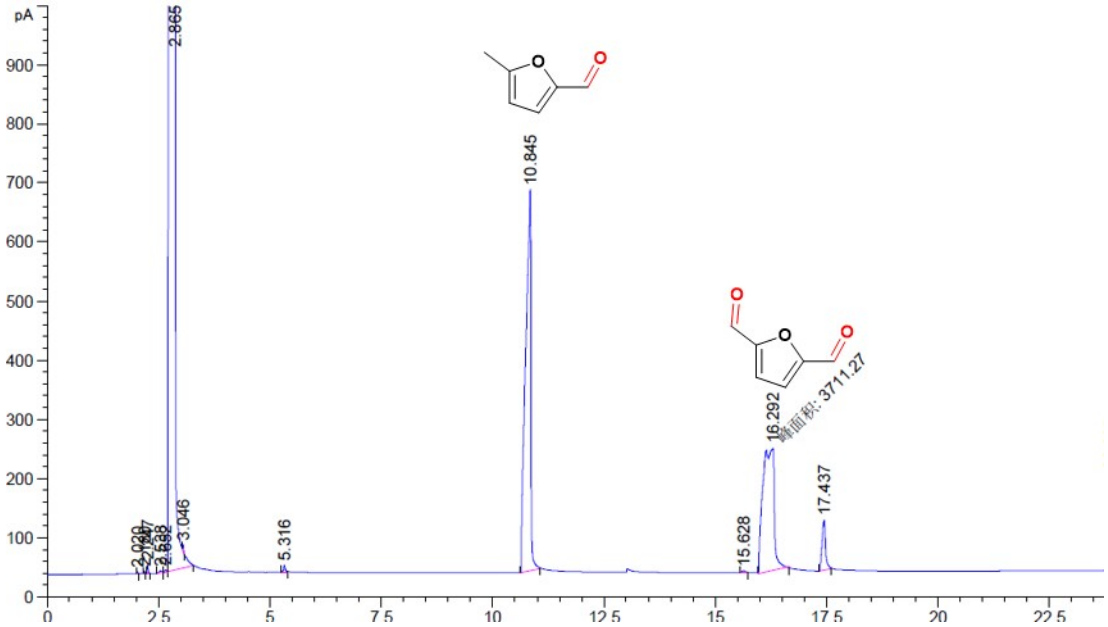


**Figure S7.** GC picture of 5-hydroxymethylfurfural disproportionation reaction product.

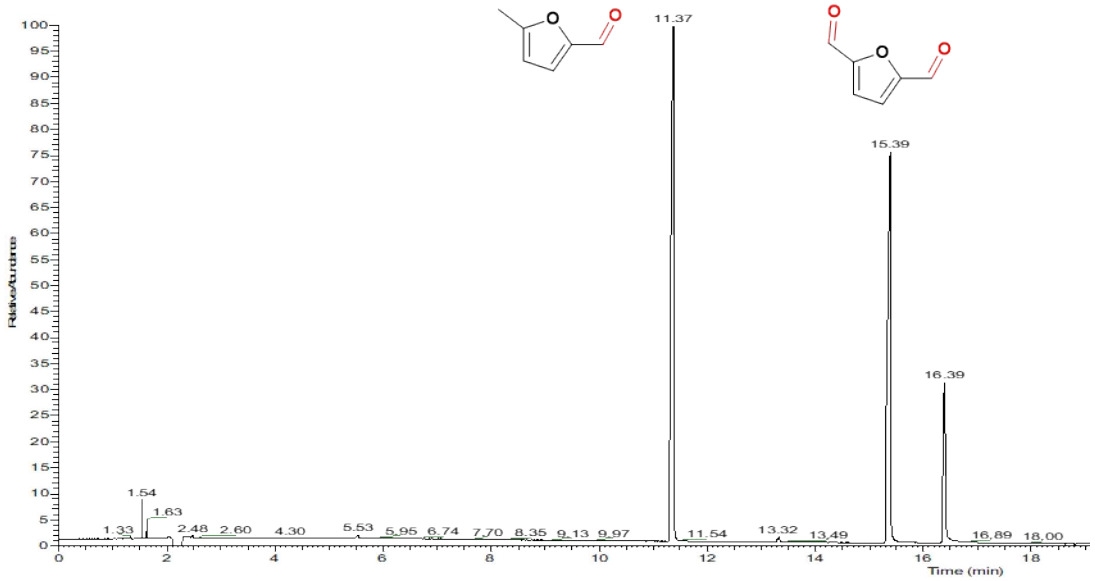


**Figure S8.** GCMS picture of 5-hydroxymethylfurfural disproportionation reaction product.

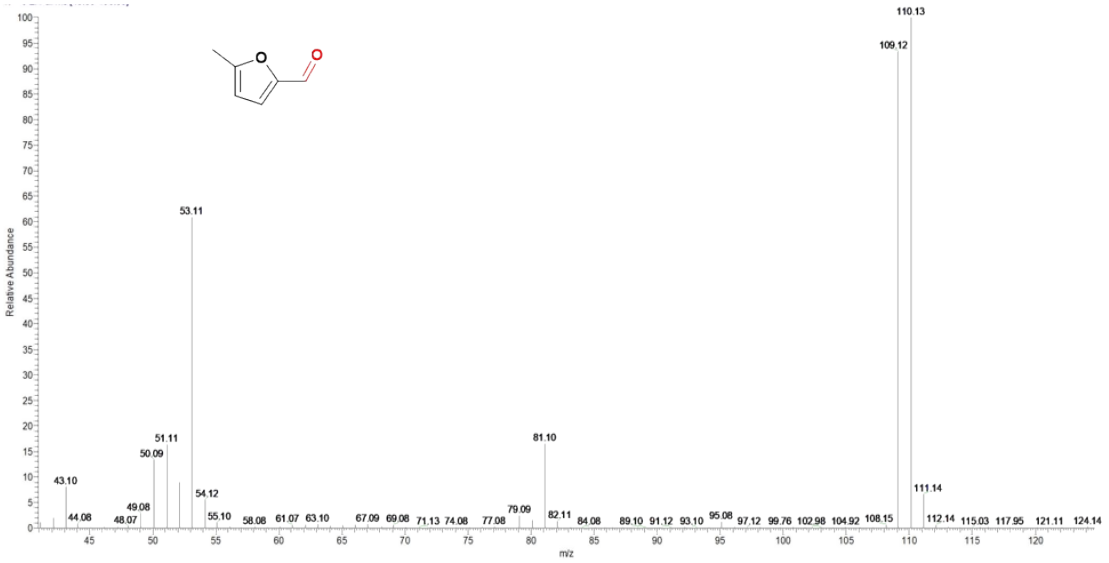


**Figure S9.** 5-methylfurfural GCMS fragment peak graph.

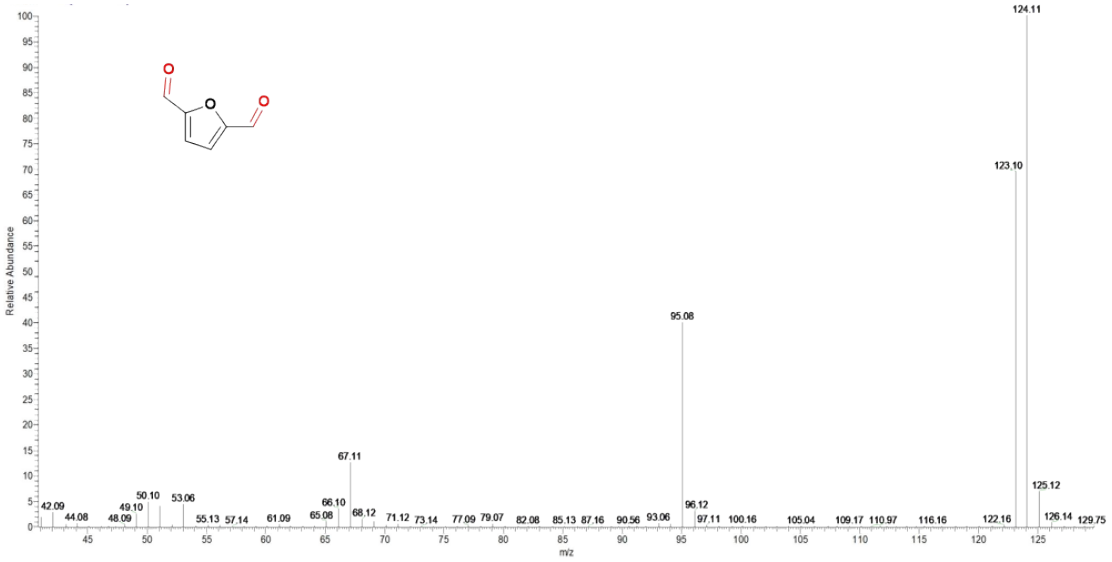


**Figure S10.** 2,5-furandicarbaldehyde GCMS fragment peak graph.

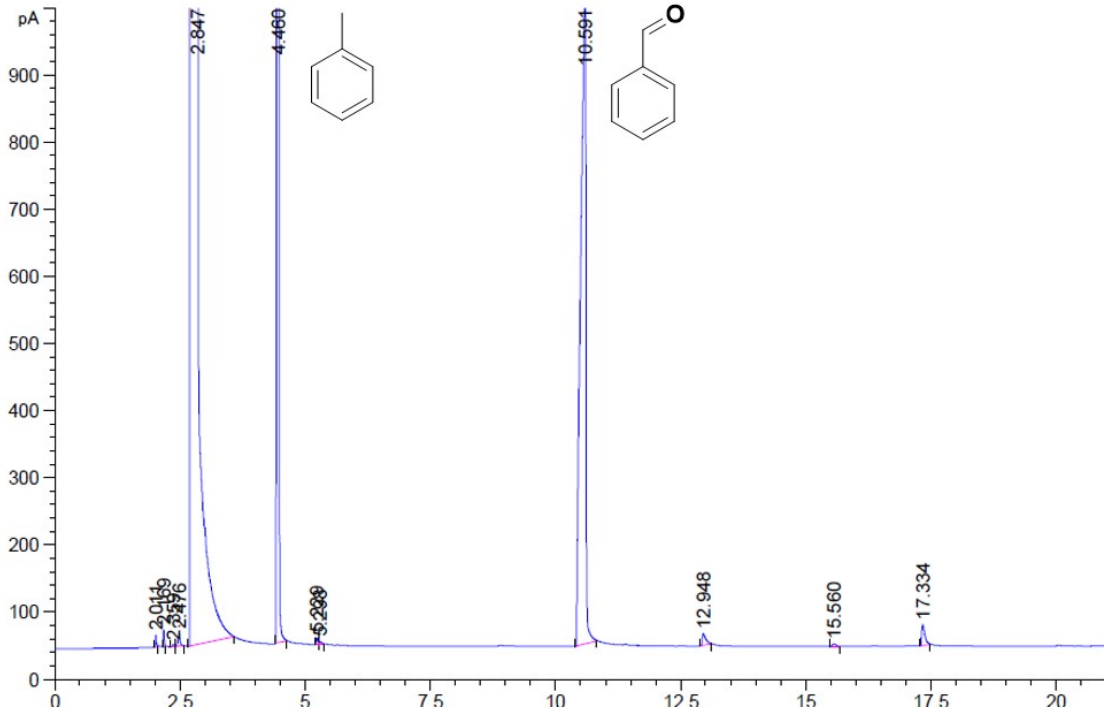


**Figure S11.** GC picture of benzyl alcohol disproportionation reaction product.

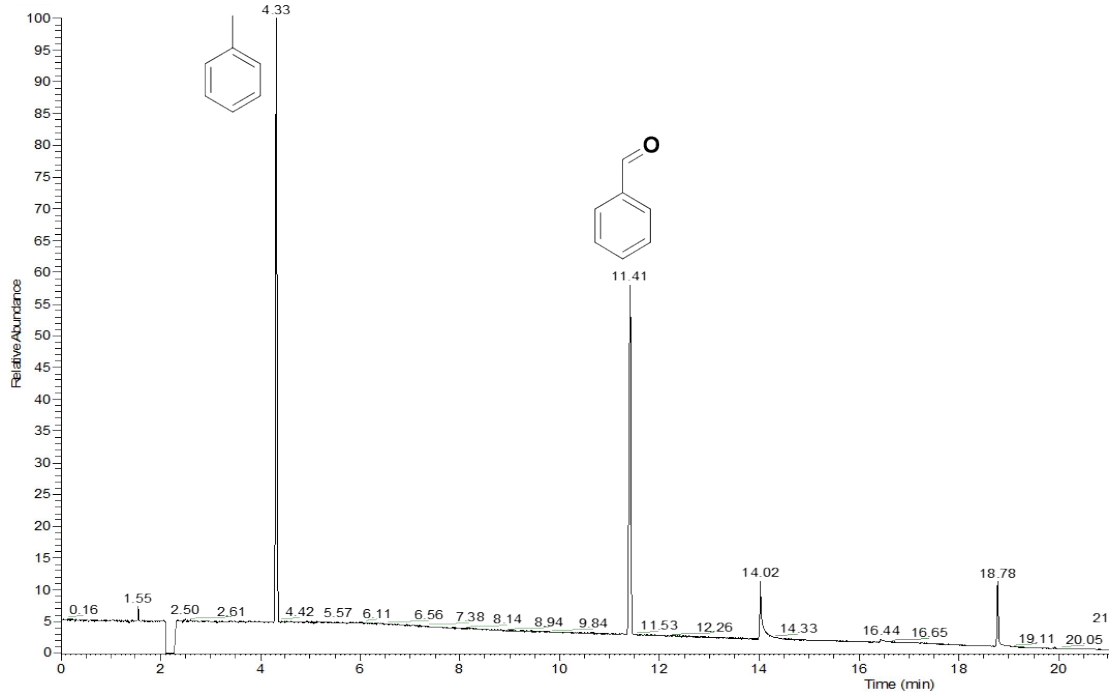


**Figure S12.** GCMS picture of benzyl alcohol disproportionation reaction product.

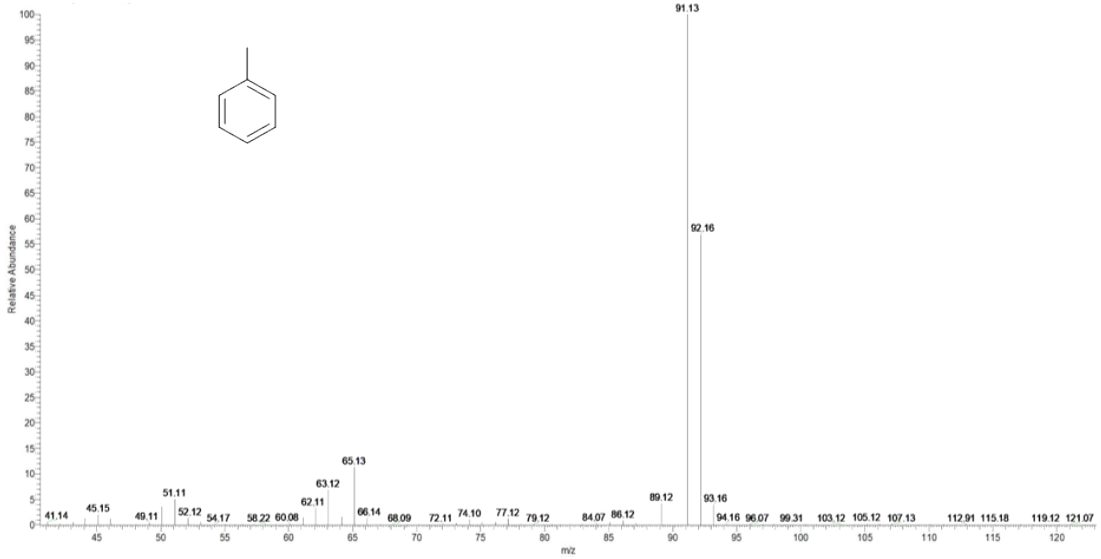


**Figure S13.** Toluene GCMS fragment peak graph.

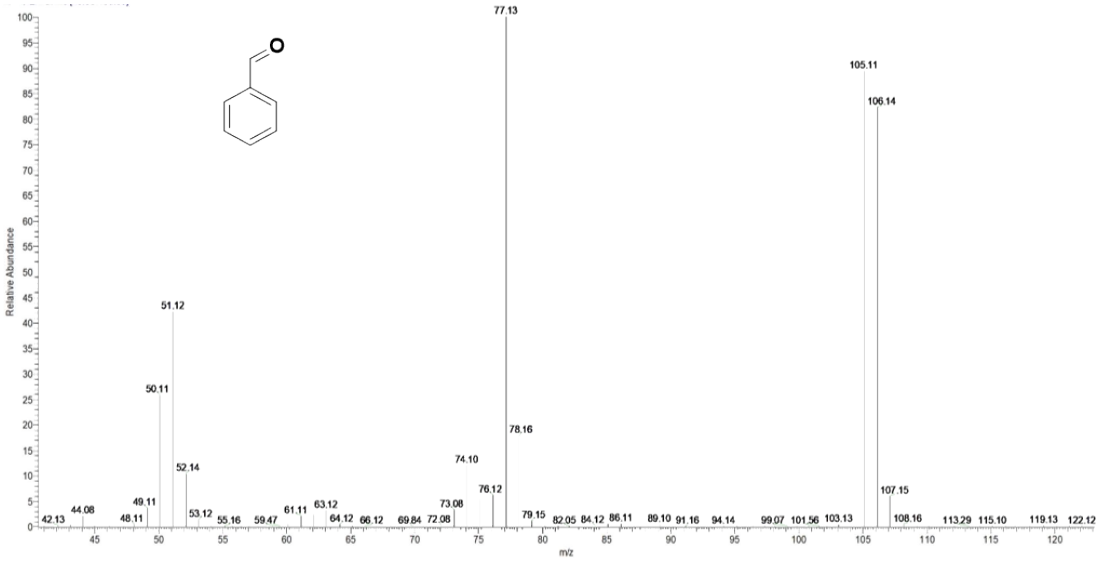


**Figure S14.** Benzaldehyde GCMS fragment peak graph.

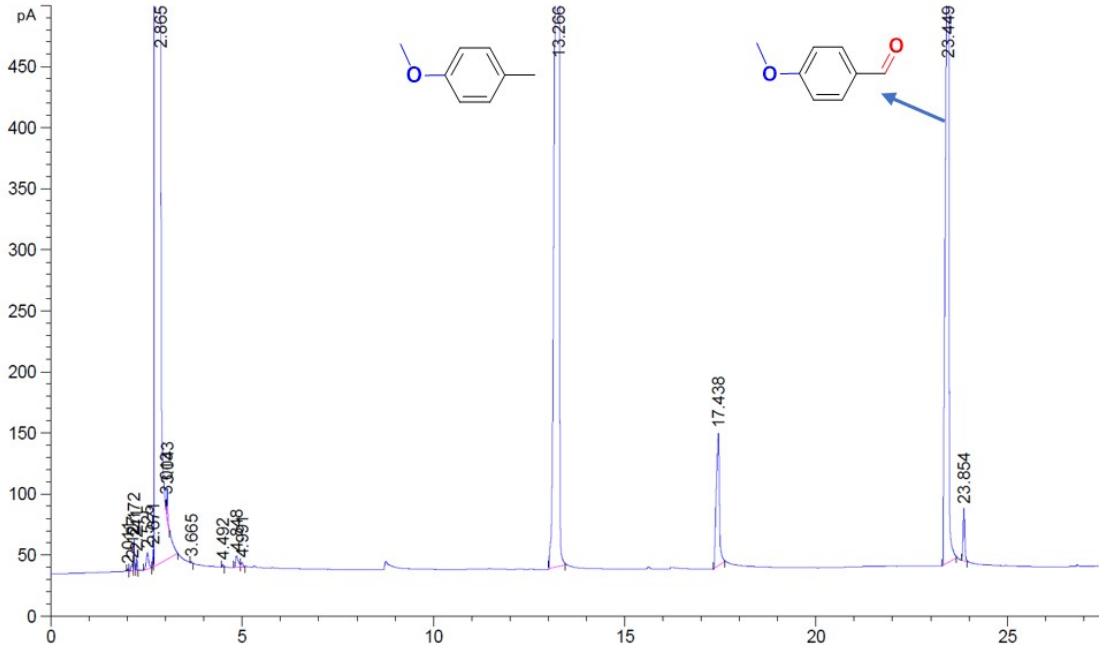


**Figure S15.** GC picture of 4-methoxybenzyl alcohol disproportionation reaction product.

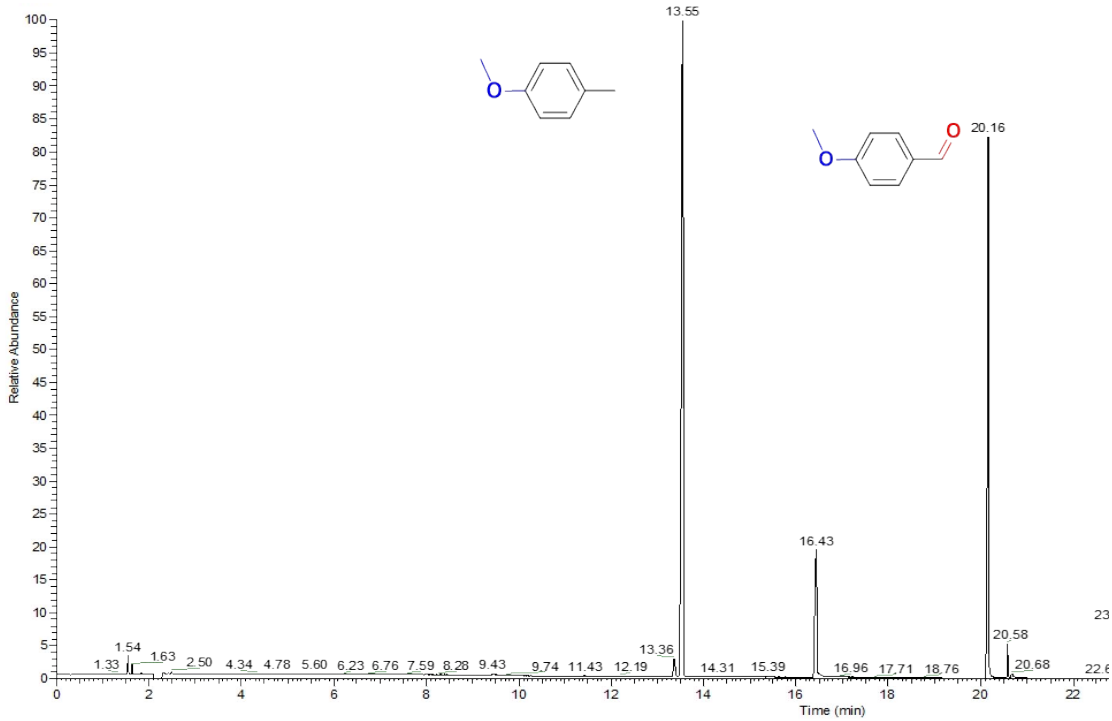


**Figure S16.** GCMS picture of 4-methoxybenzyl alcohol disproportionation reaction product.

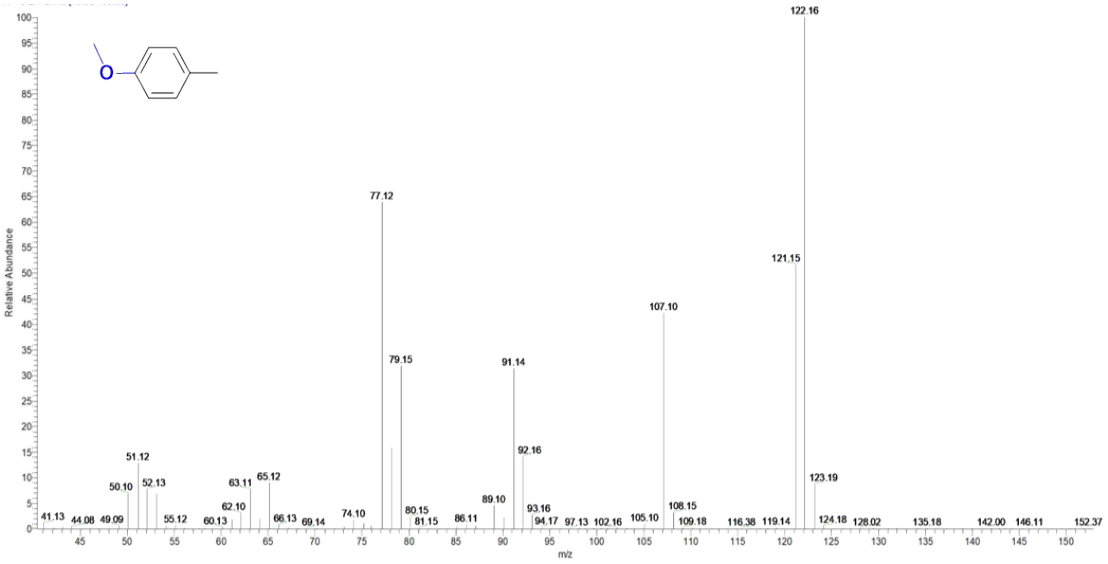


**Figure S17.** 4-Methylanisole GCMS fragment peak graph.

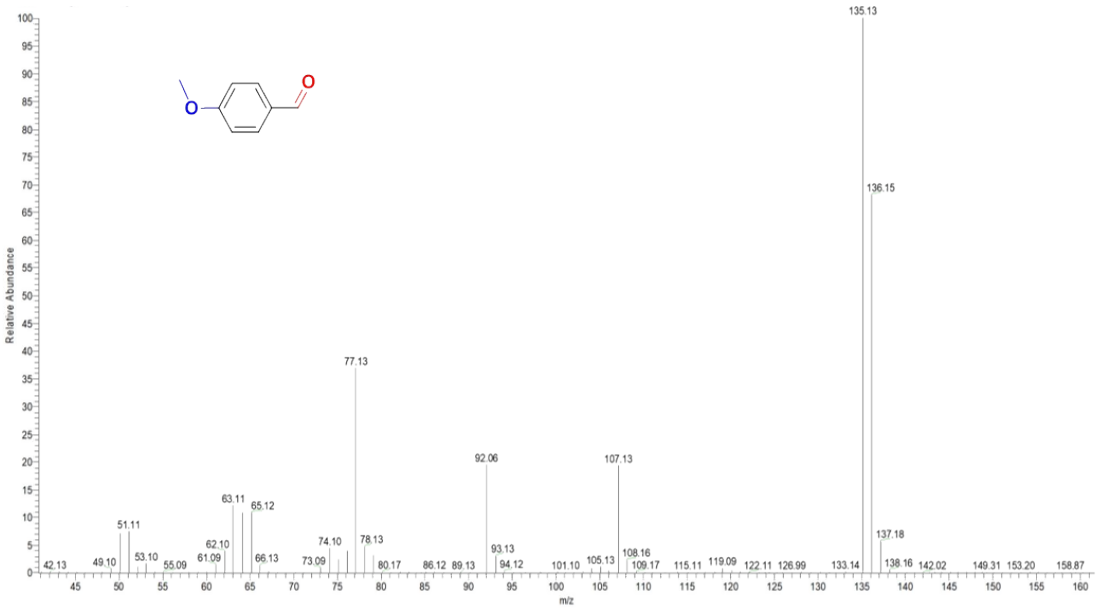


**Figure S18.** p-Anisaldehyde GC-MS fragment peak graph.

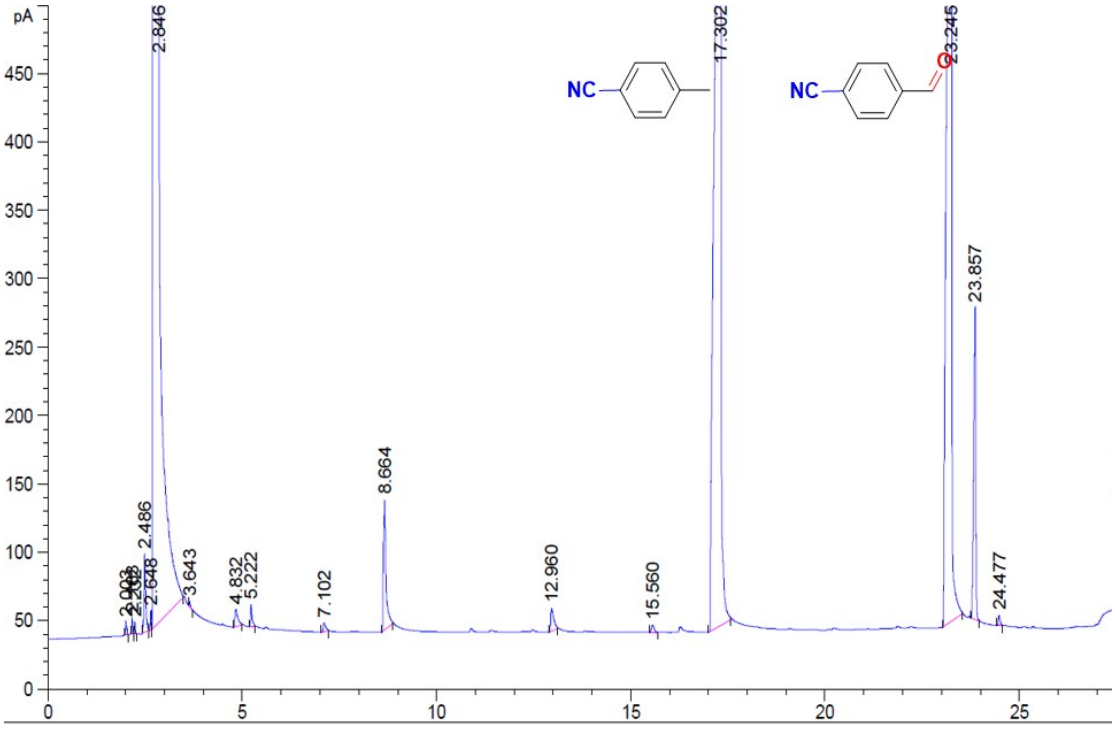


**Figure S19.** GC picture of 4-cyanobenzyl alcohol disproportionation reaction product.

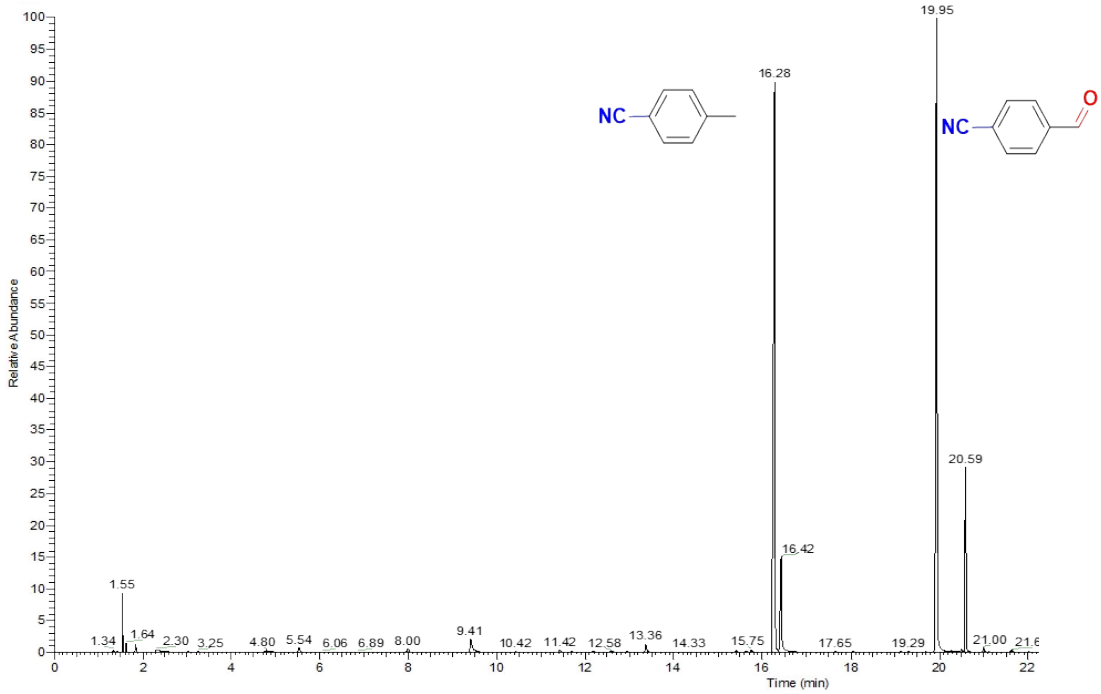


**Figure S20.** GCMS picture of 4-cyanobenzyl alcohol disproportionation reaction product.

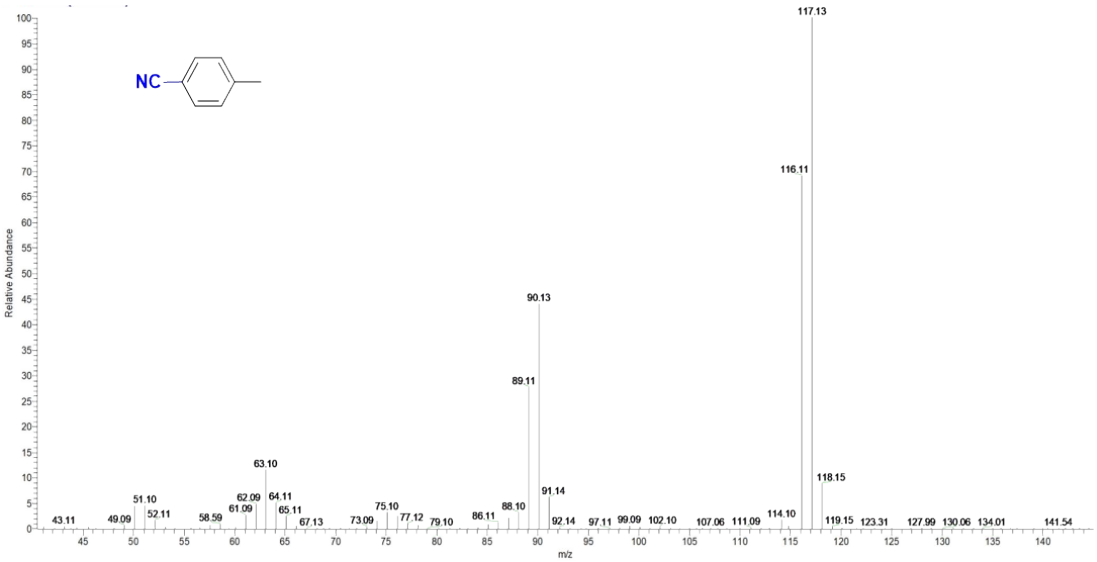


**Figure S21.** p-Tolunitrile GCMS fragment peak graph.

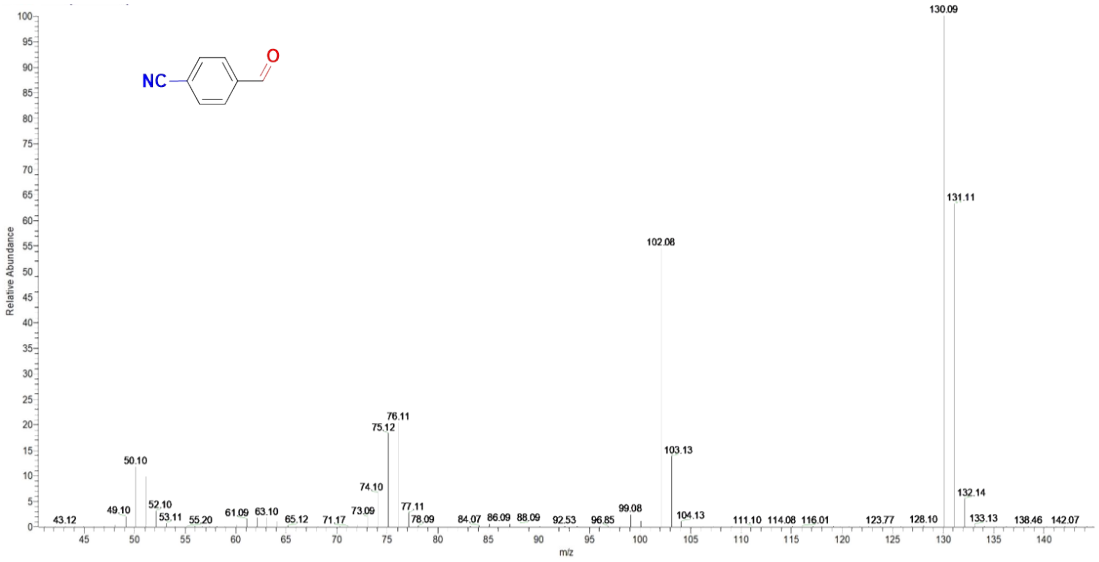


**Figure S22.** 4-Cyanobenzaldehyde GCMS fragment peak graph.

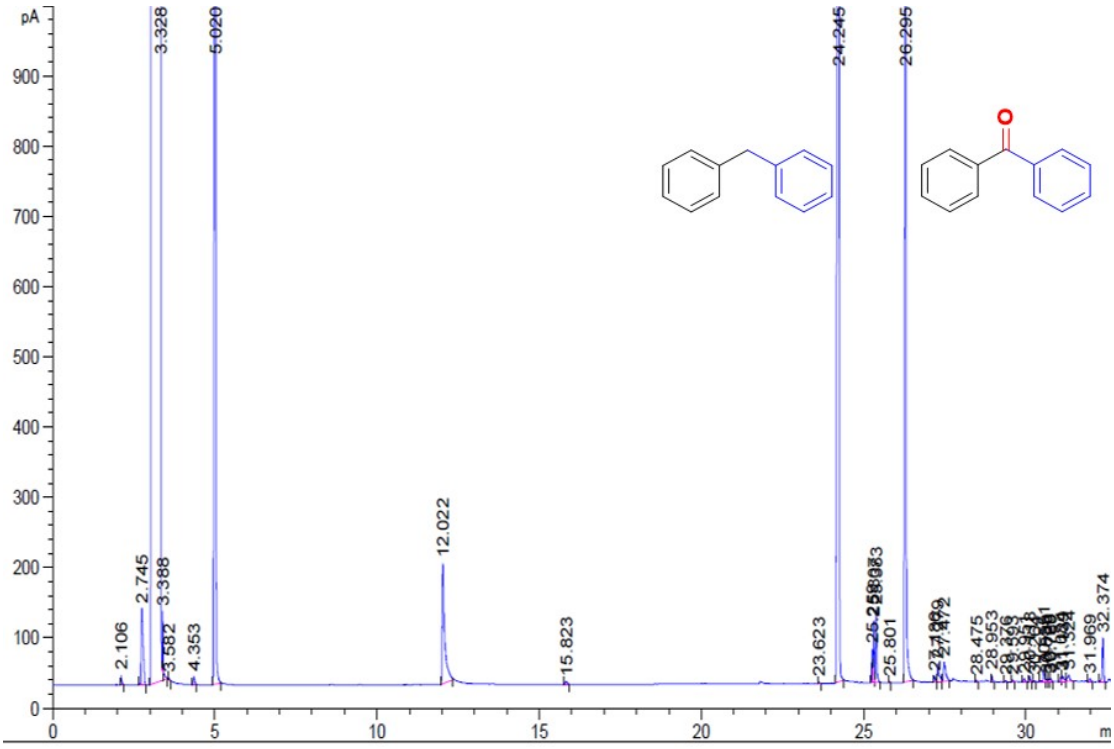


**Figure S23.** GC picture of benzhydrol disproportionation reaction product.

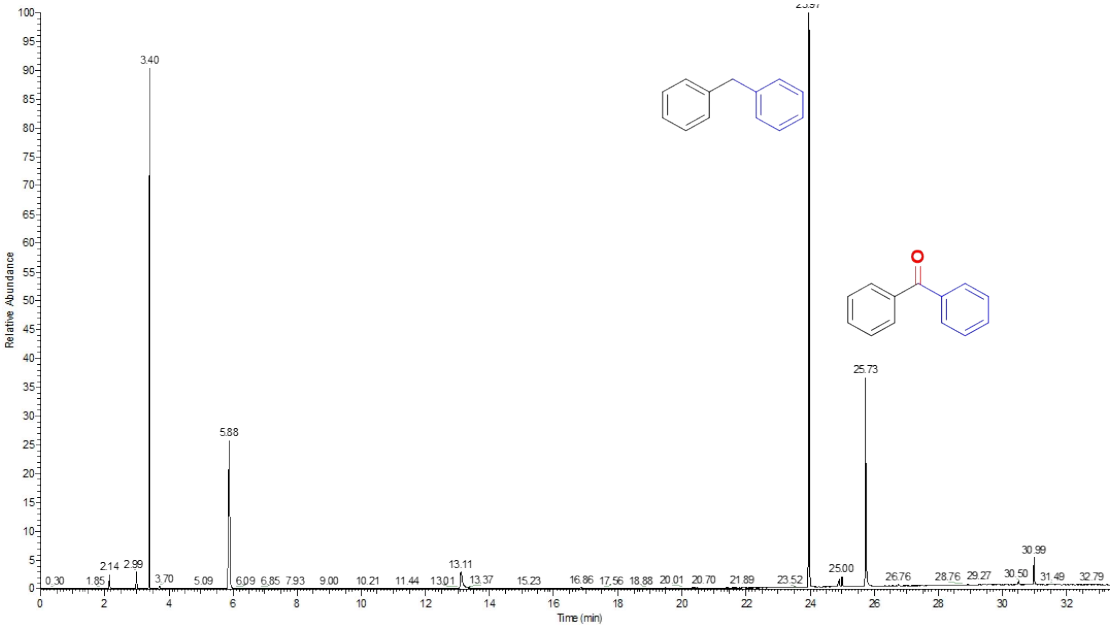


**Figure S24.** GCMS picture of benzhydrol disproportionation reaction product.

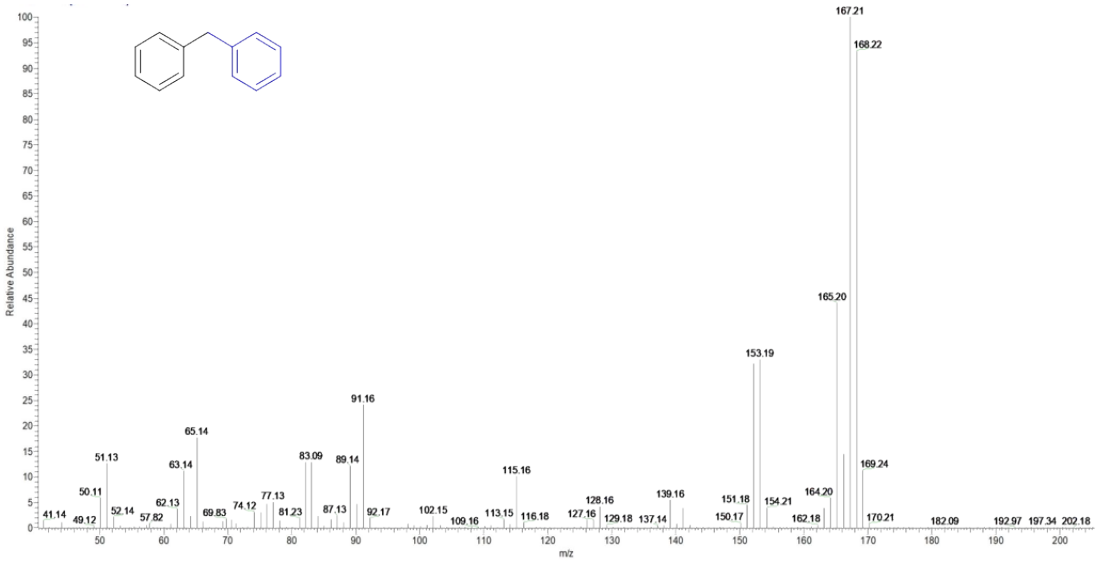


**Figure S25.** Diphenylmethane GCMS fragment peak graph.

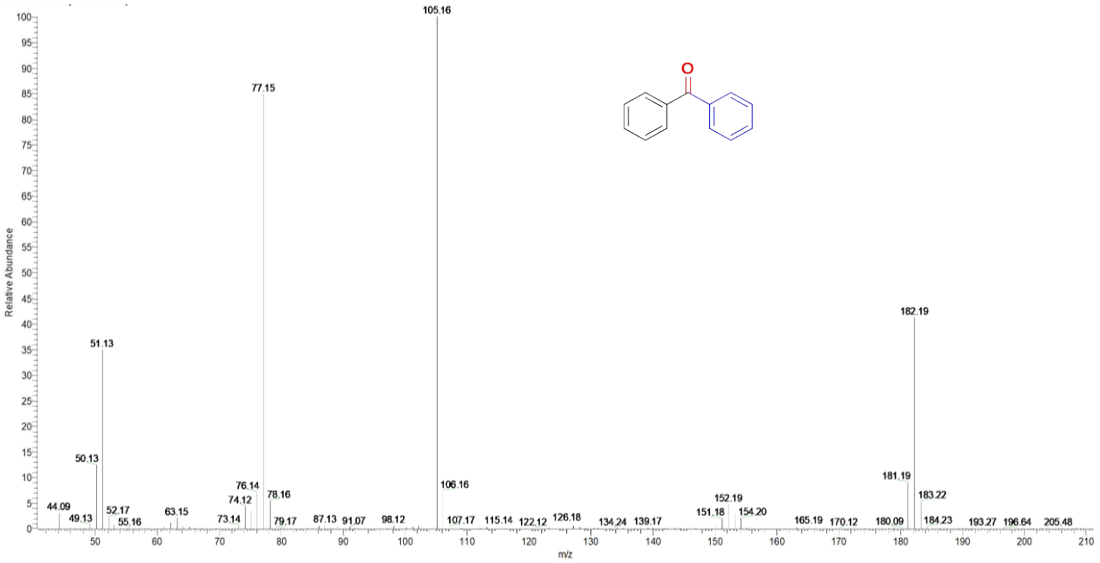


**Figure S26.** Benzophenone GCMS fragment peak graph.

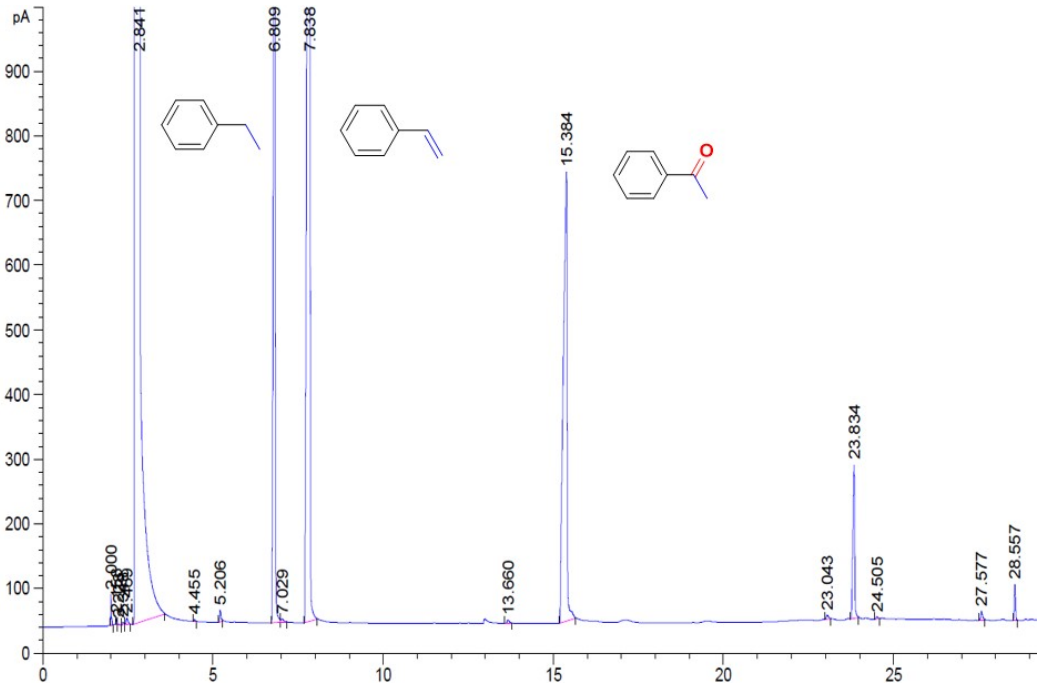


**Figure S27.** GC picture of DL-1-Phenethylalcohol disproportionation reaction product.

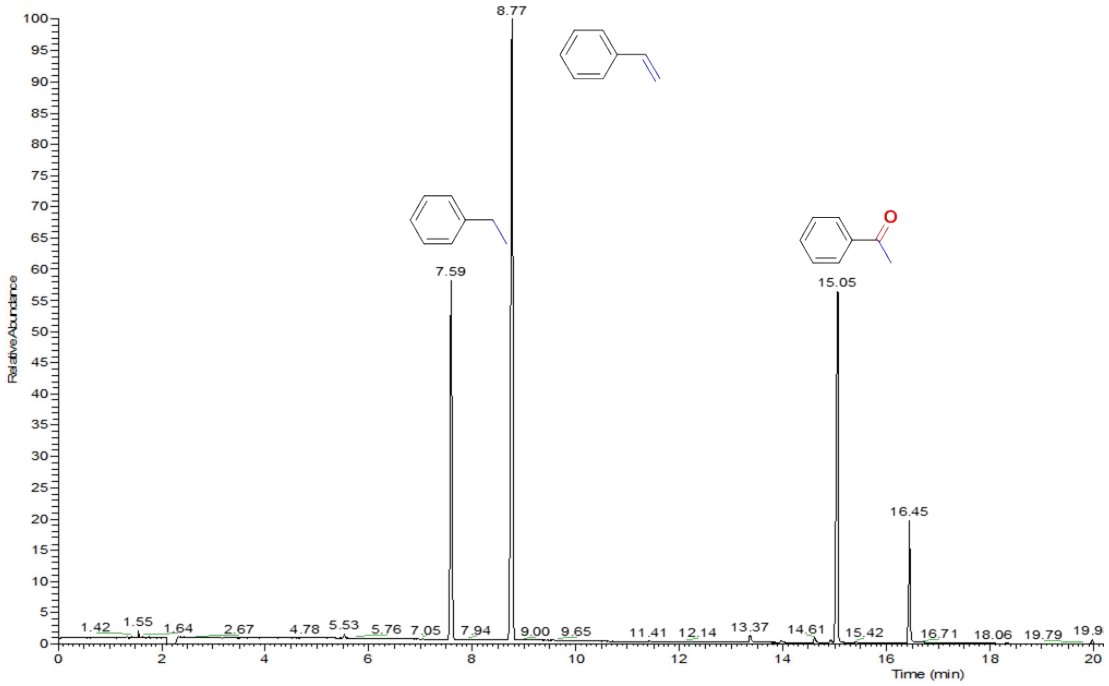


**Figure S28.** GCMS picture of DL-1-Phenethylalcohol disproportionation reaction product.

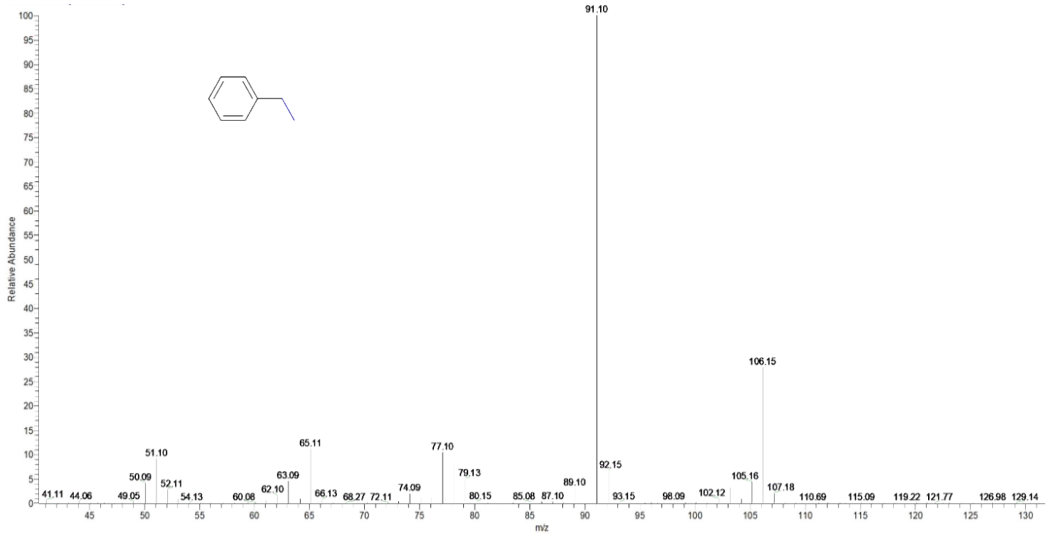


**Figure S29.** Ethylbenzene GCMS fragment peak graph.

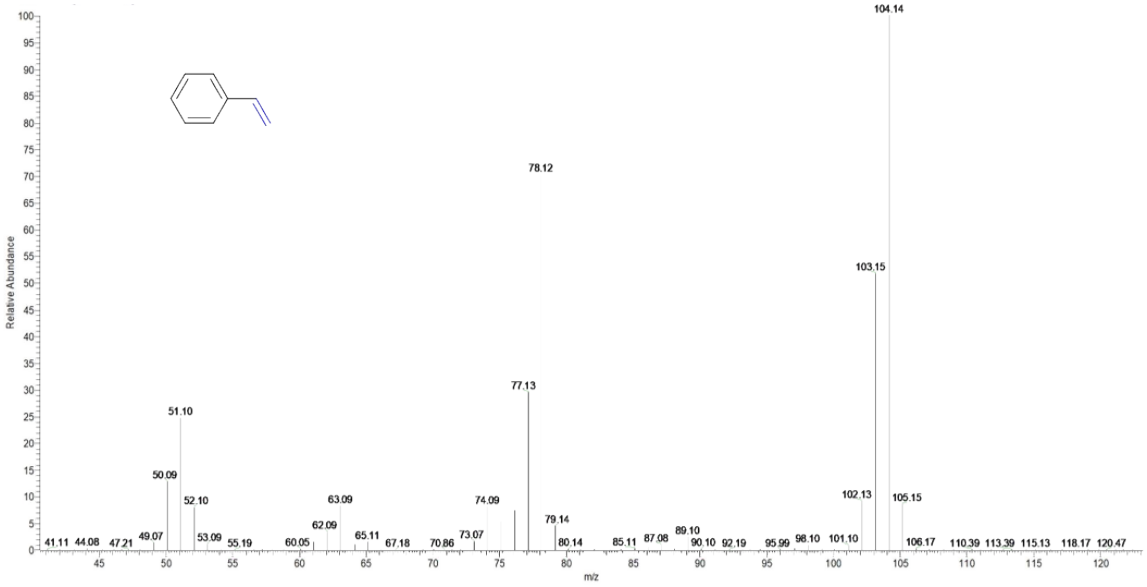


**Figure S30.** Styrene GCMS fragment peak graph.

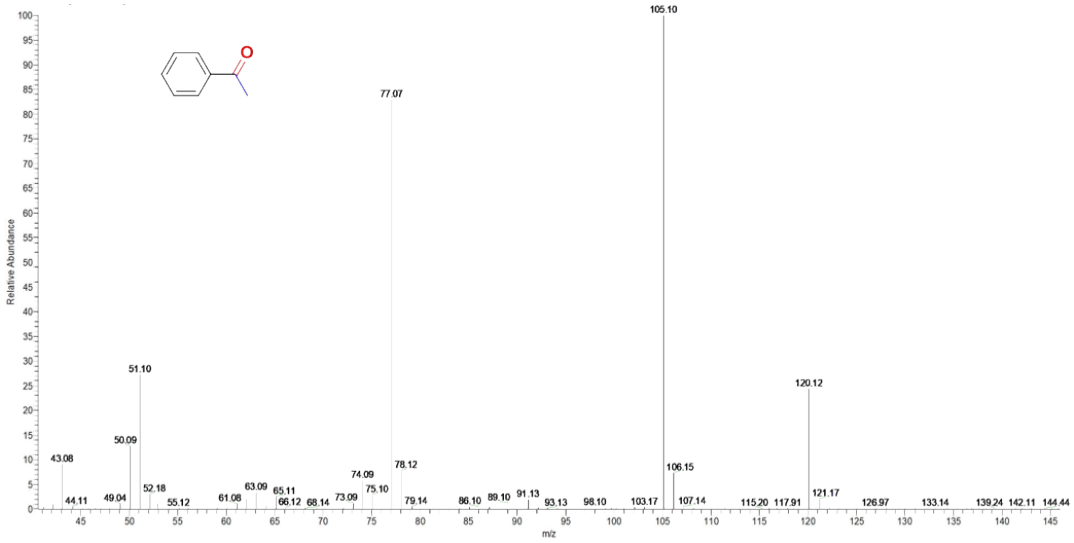


**Figure S31.** Acetophenone GCMS fragment peak graph.

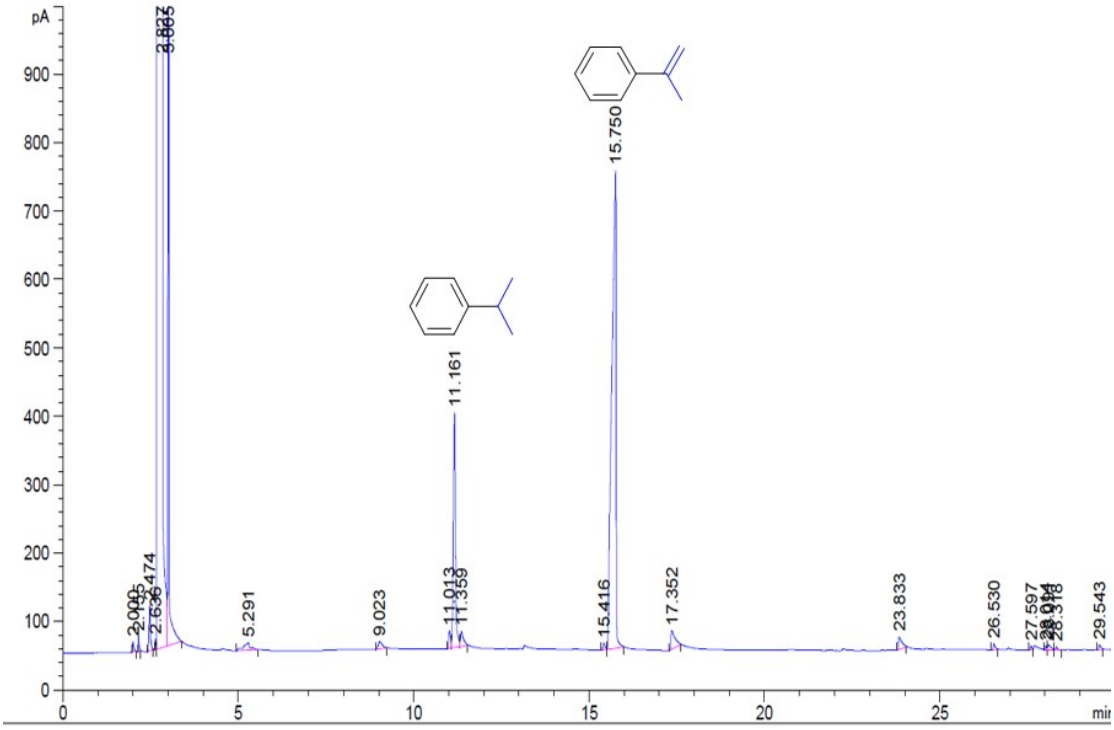


**Figure S32.** GC picture of 2-phenyl-2-propanol disproportionation reaction product.

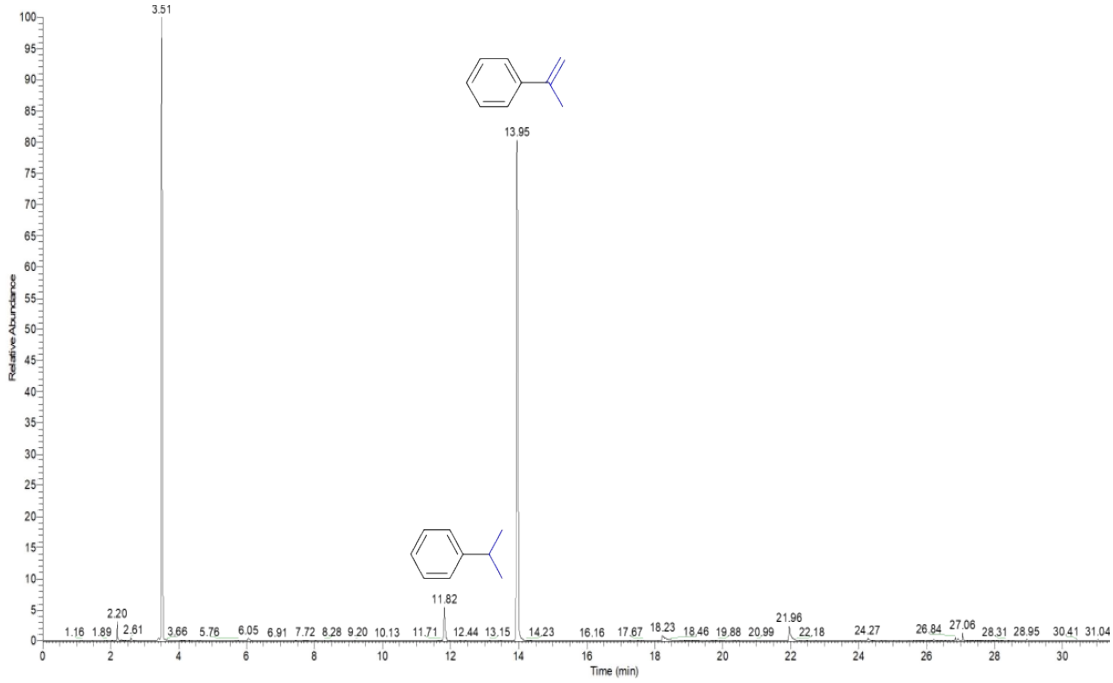


**Figure S33.** GCMS picture of 2-phenyl-2-propanol disproportionation reaction product.

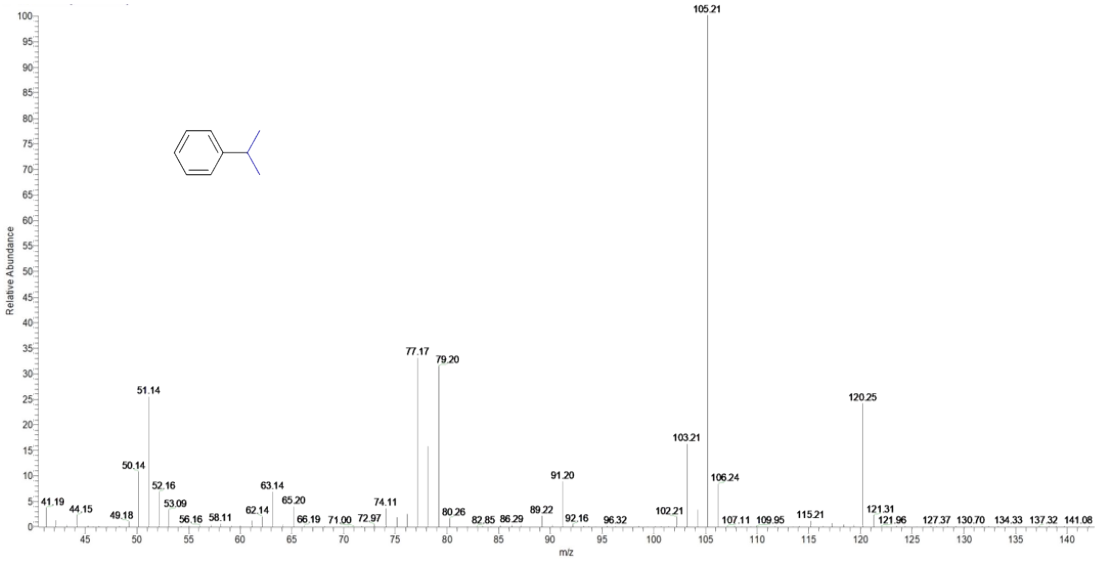


**Figure S34.** Cumene GCMS fragment peak graph.

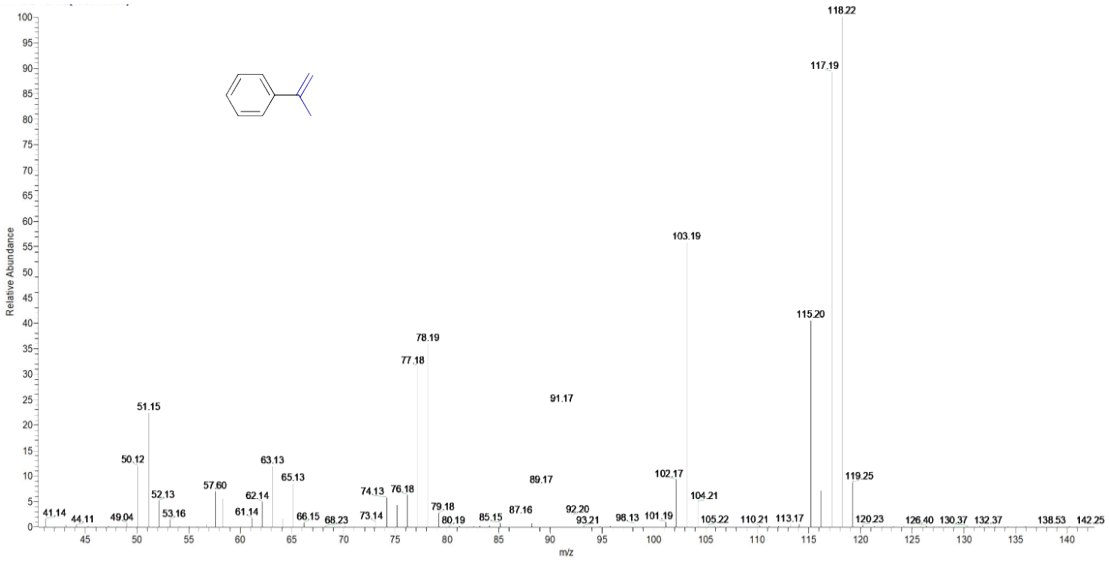


**Figure S35.** 2-Phenyl-1-propene GCMS fragment peak graph.

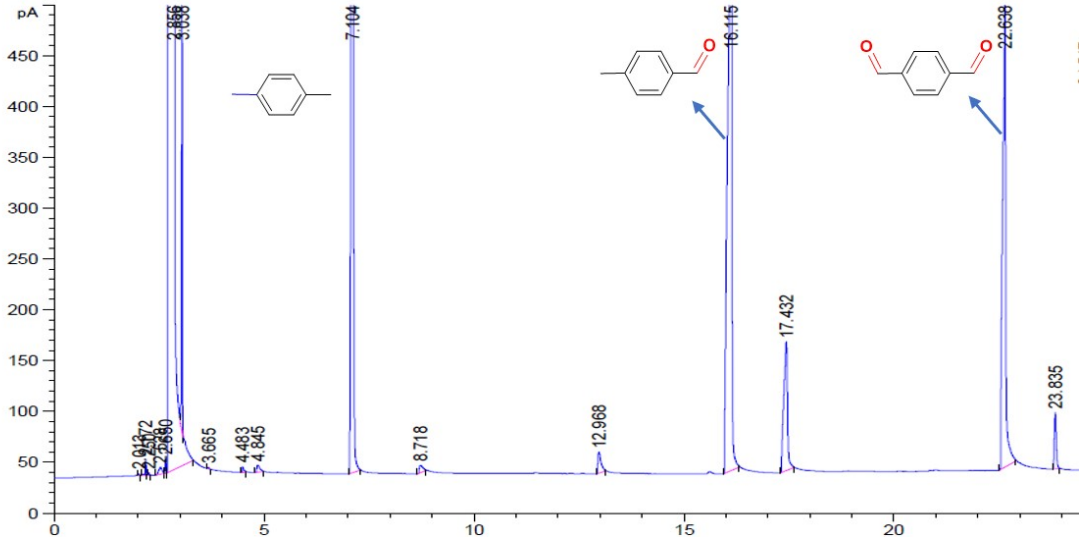

**Figure S36.** GC picture of 1,4-benzenedimethanol disproportionation reaction product.

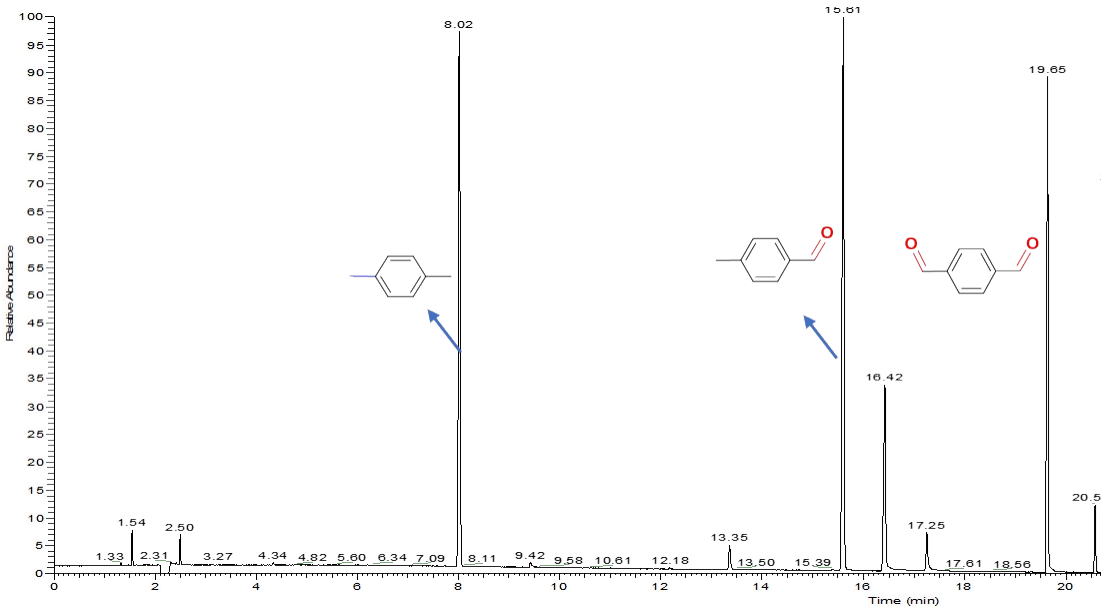


**Figure S37.** GCMS picture of 1,4-benzenedimethanol disproportionation reaction product.

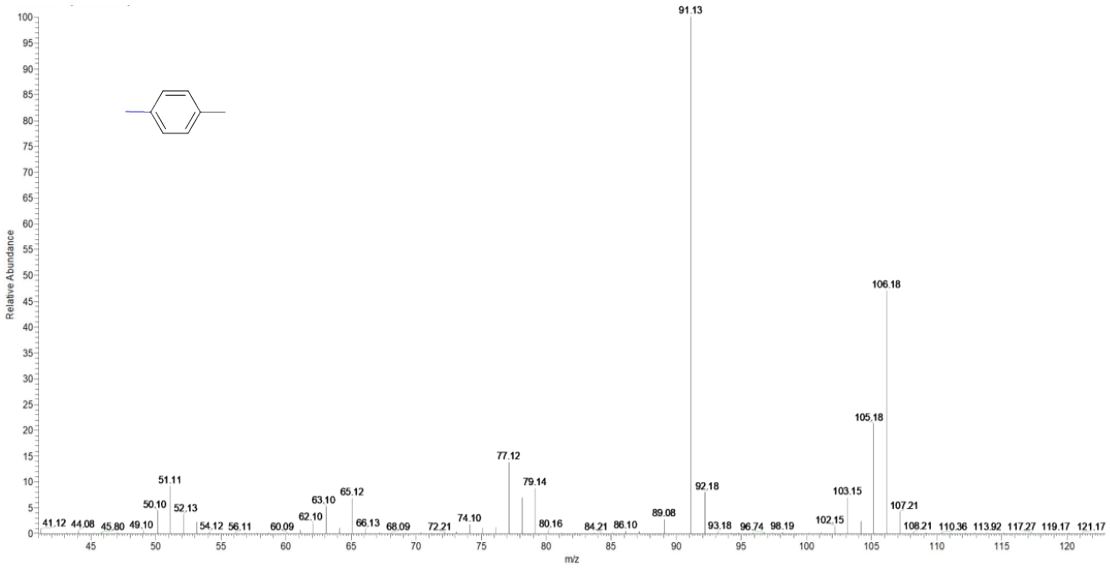


**Figure S38.** P-xylene GCMS fragment peak graph.

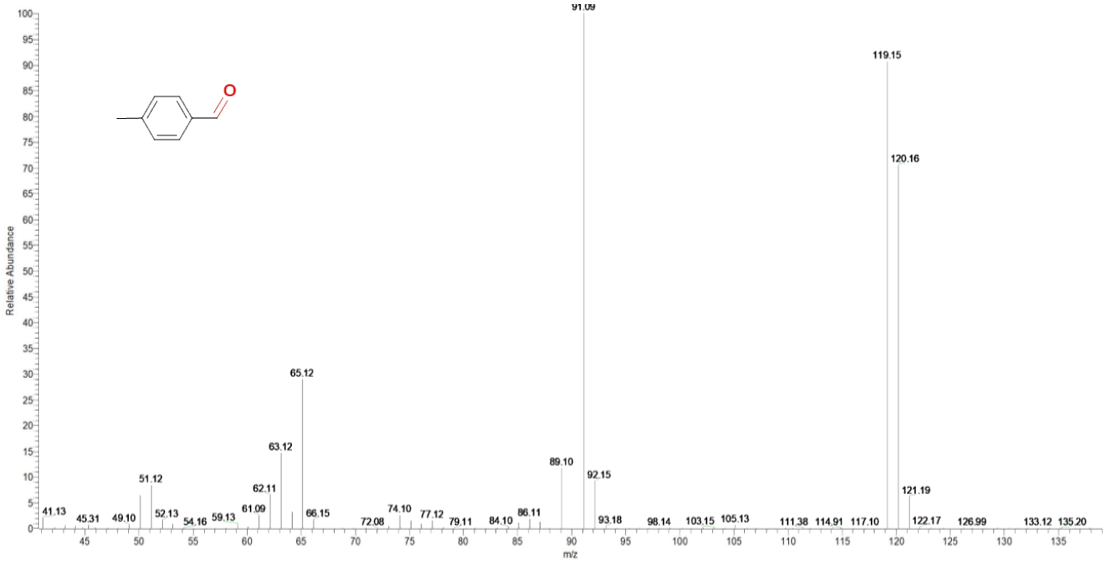


**Figure S39.** p-Tolualdehyde GCMS fragment peak graph.

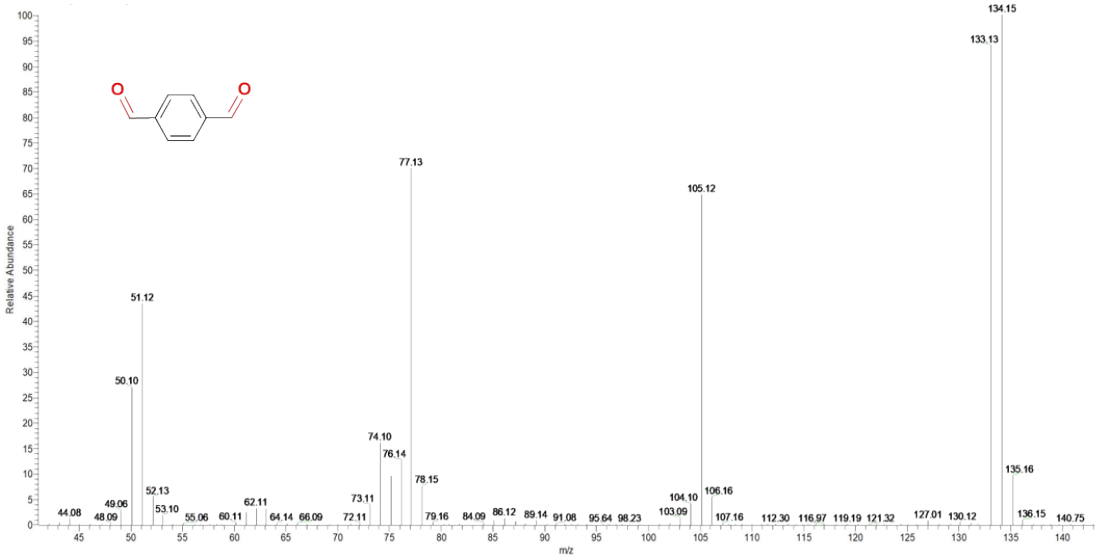


**Figure S40.** Terephthalaldehyde GCMS fragment peak graph.

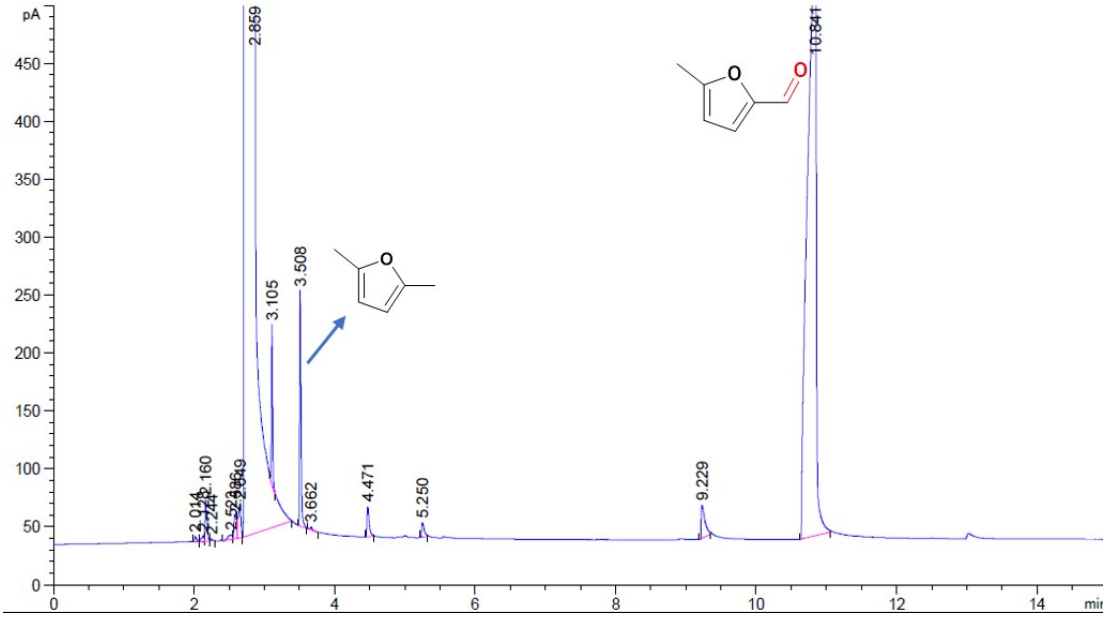


**Figure S41.** GC picture of 2,5-furandimethanol disproportionation reaction product.

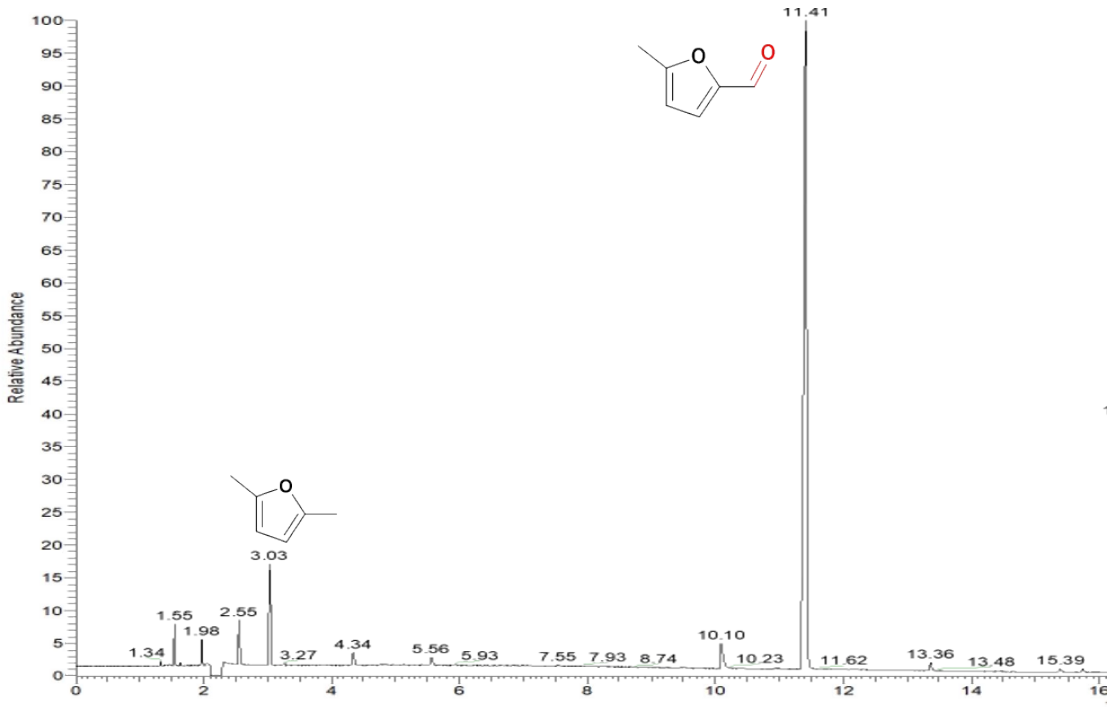


**Figure S42.** GCMS picture of 2,5-furandimethanol disproportionation reaction product.

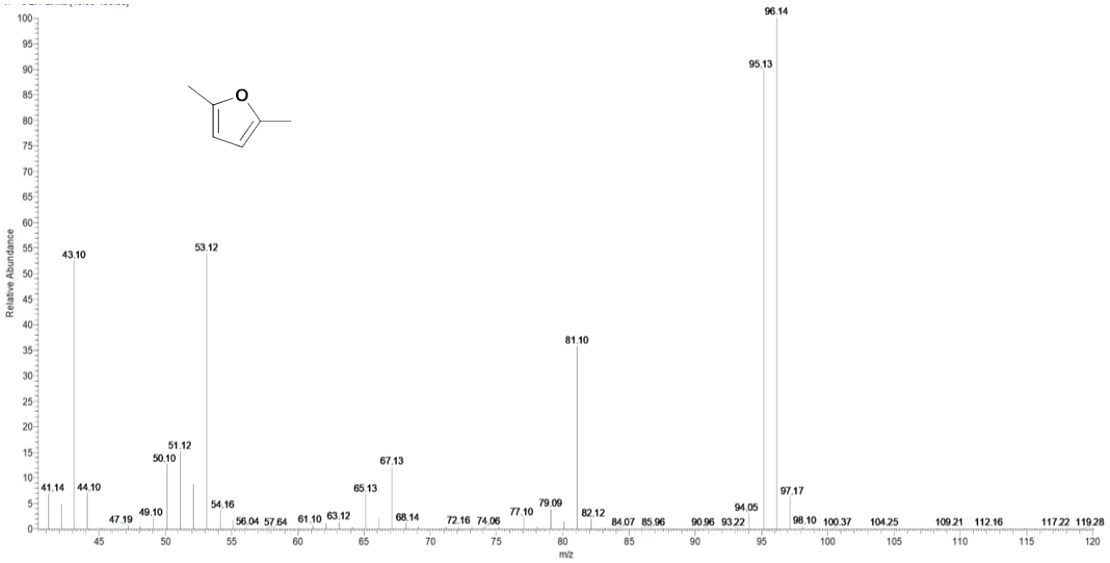


**Figure S43.** 2,5-Dimethylfuran GCMS fragment peak graph.

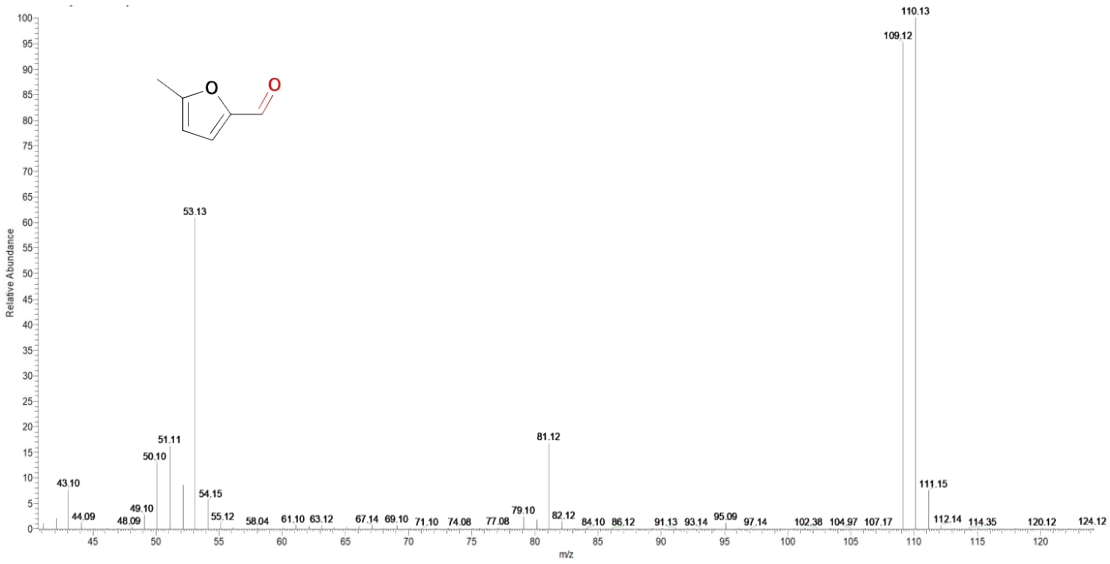


**Figure S44.** 5-methylfurfural GCMS fragment peak graph.

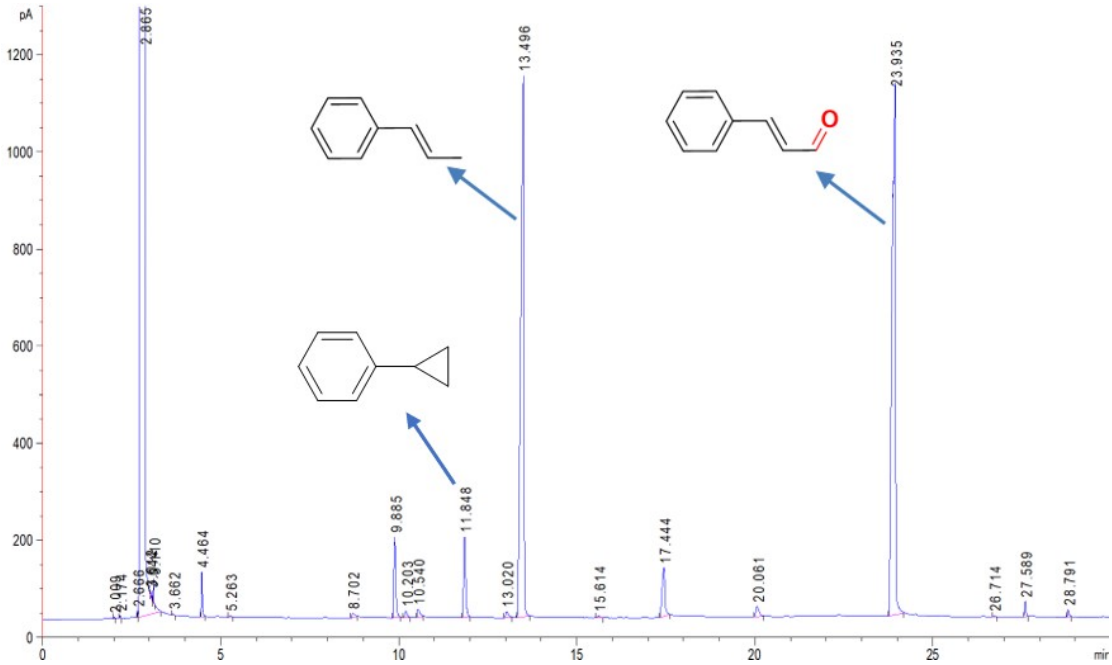


**Figure S45.** GC picture of cinnamyl alcohol disproportionation reaction product.

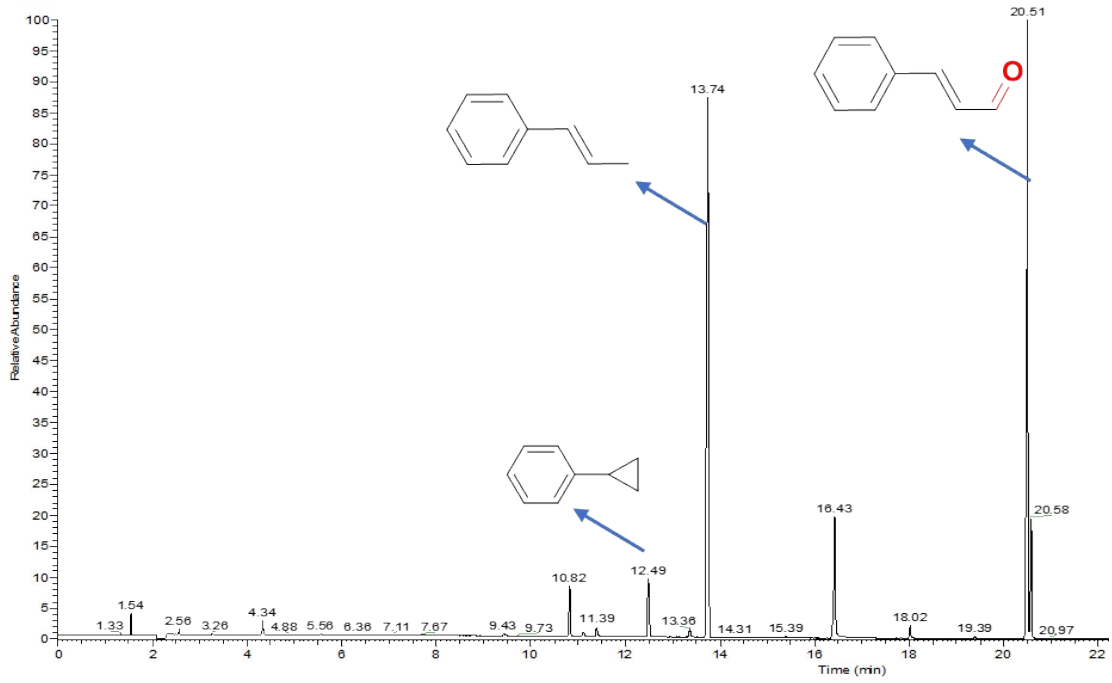


**Figure S46.** GCMS picture of cinnamyl alcohol disproportionation reaction product.

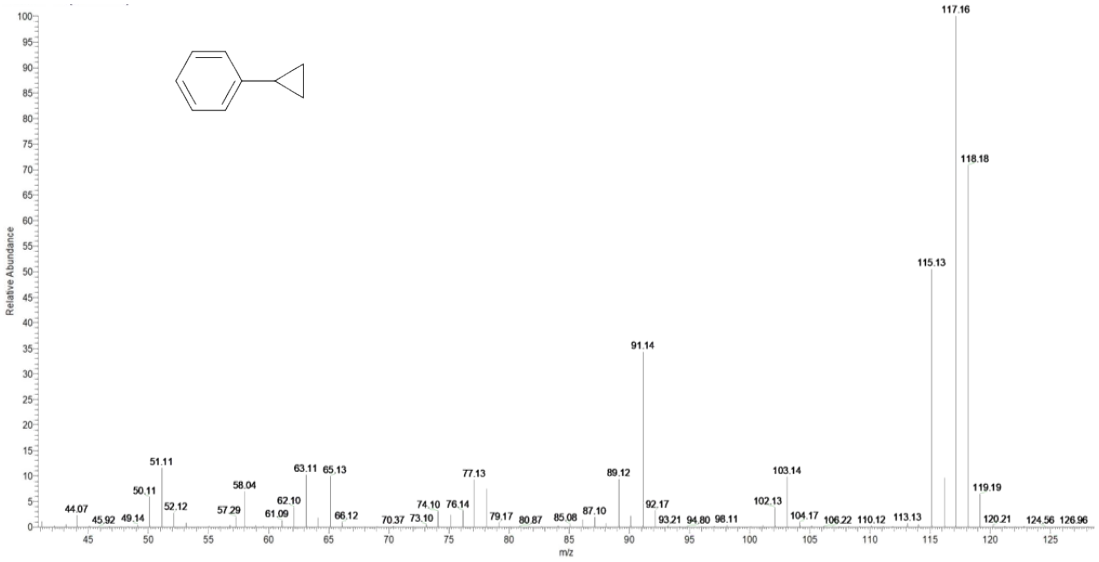


**Figure S47.** Cyclopropylbenzen GCMS fragment peak graph.

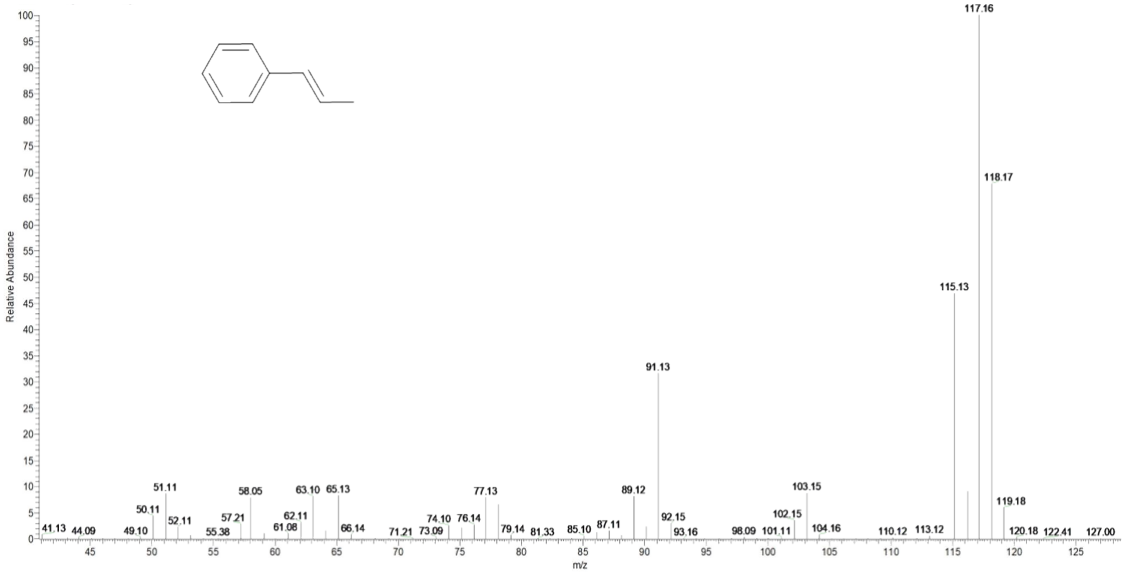


**Figure S48.** β-Methylstyrene GCMS fragment peak graph.

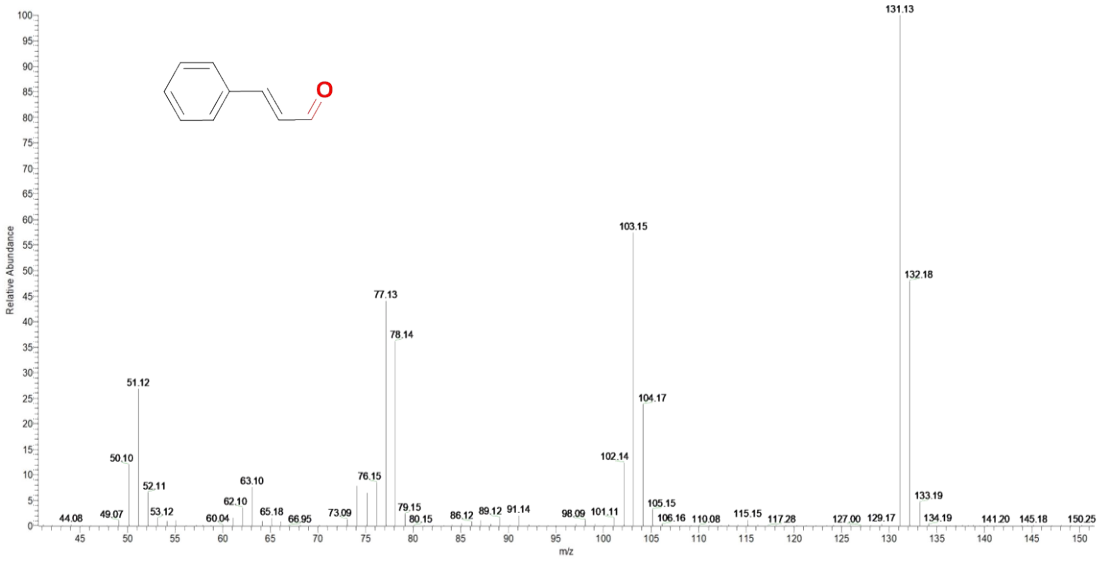


**Figure S49.** Cinnamaldehyde GCMS fragment peak graph.

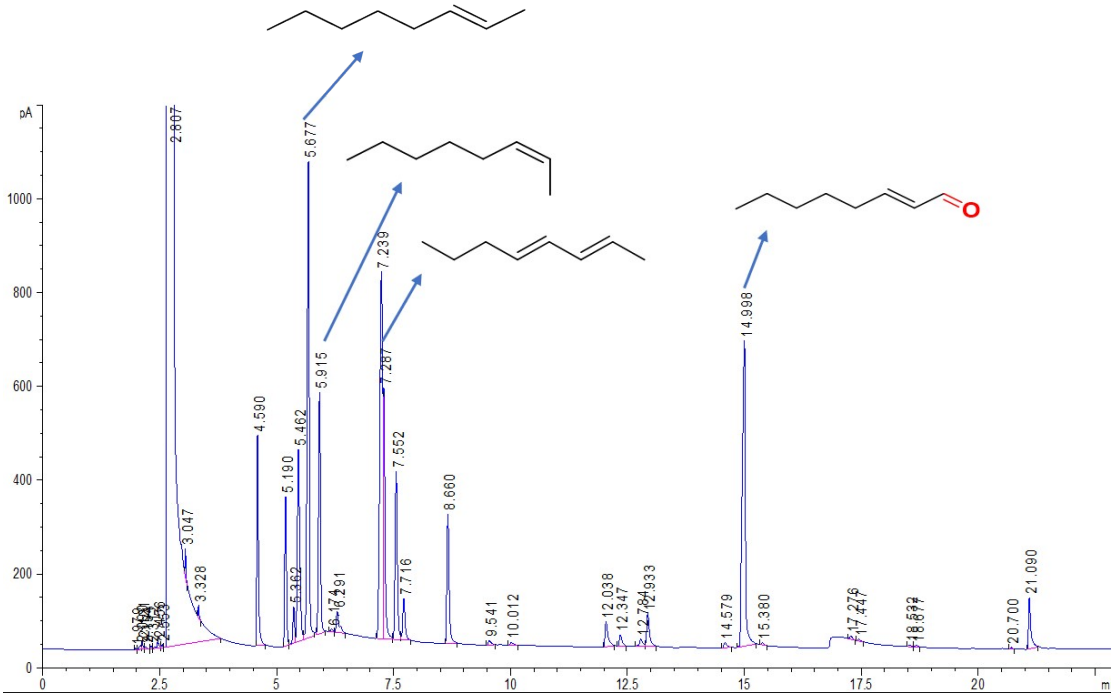


**Figure S50.** GC picture of trans-2-octenol disproportionation reaction product.

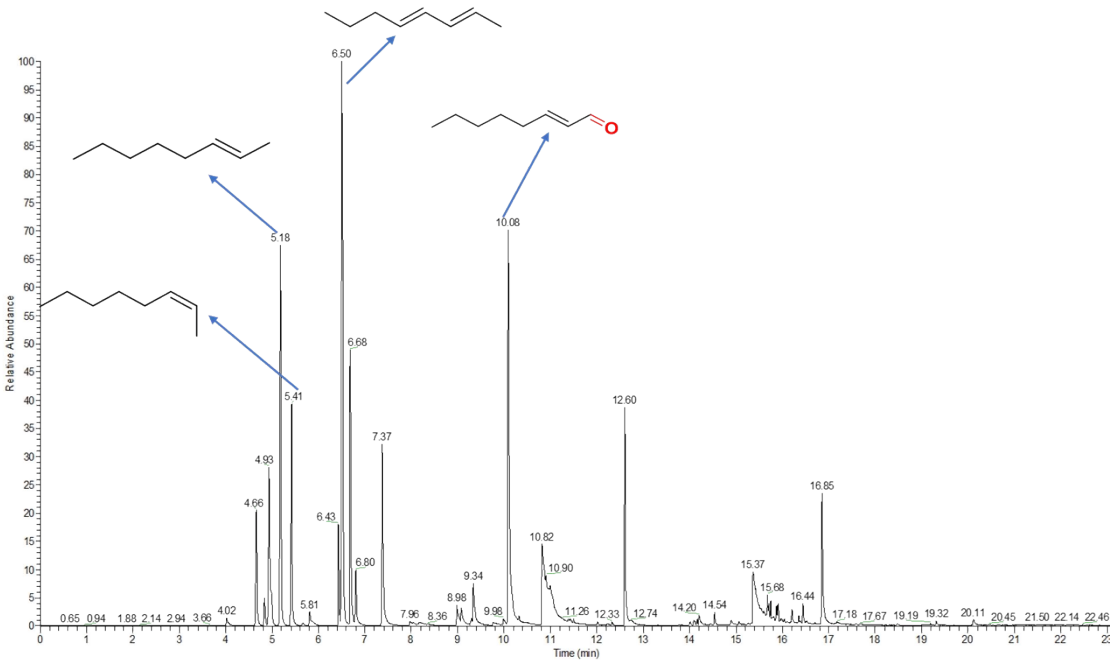


**Figure S51.** GCMS picture of trans-2-octenol disproportionation reaction product.

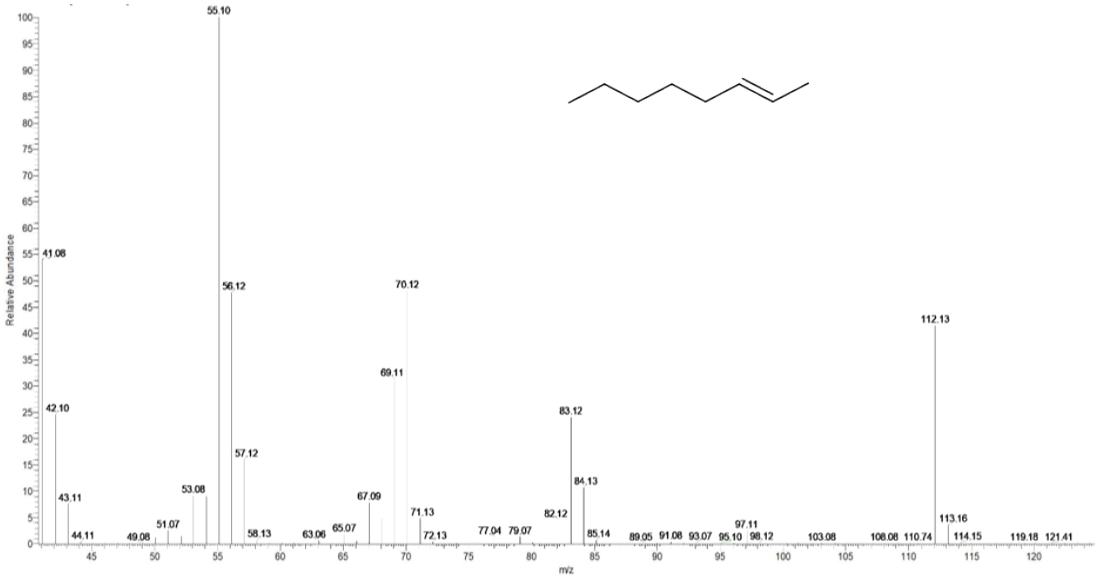


**Figure S52.** Trans-2-octene GCMS fragment peak graph.

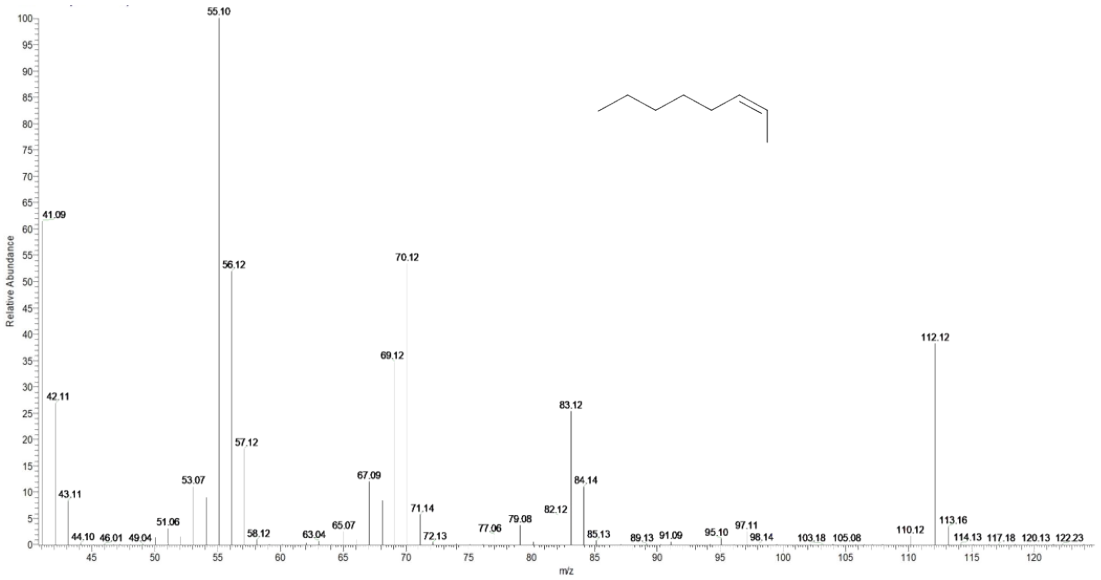


**Figure S53.** Cis-2-octene GCMS fragment peak graph.

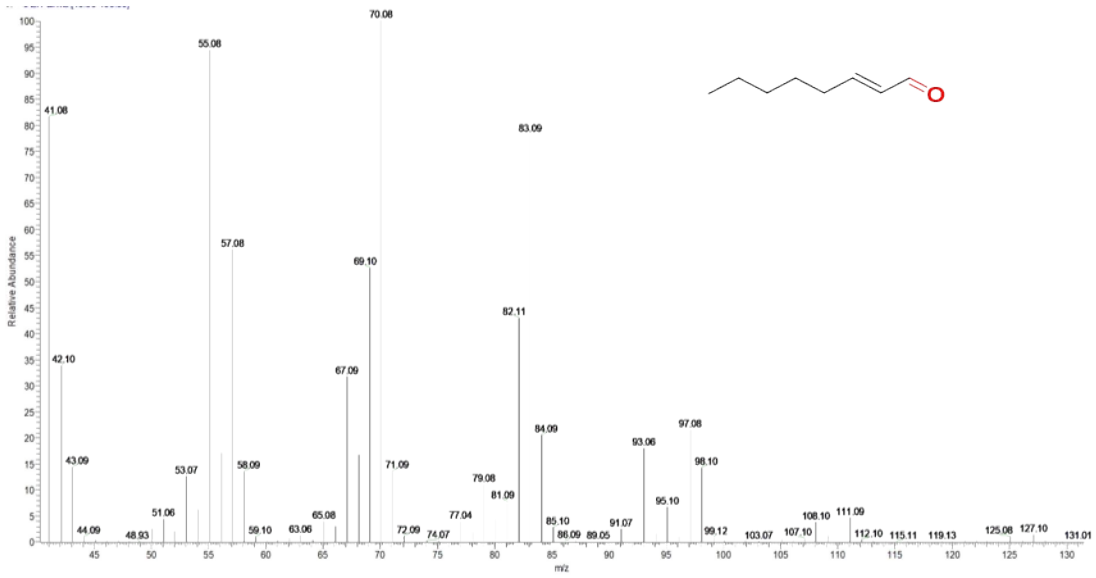


**Figure S54.** 2-Octenal GCMS fragment peak graph.

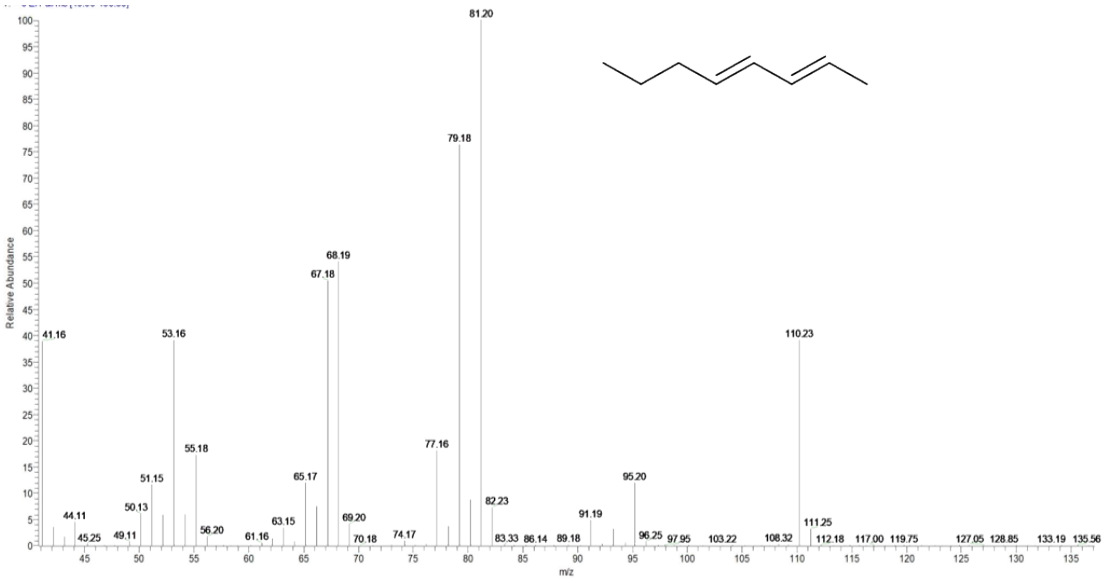


**Figure S55.** 2,4-Dioctene GCMS fragment peak graph.

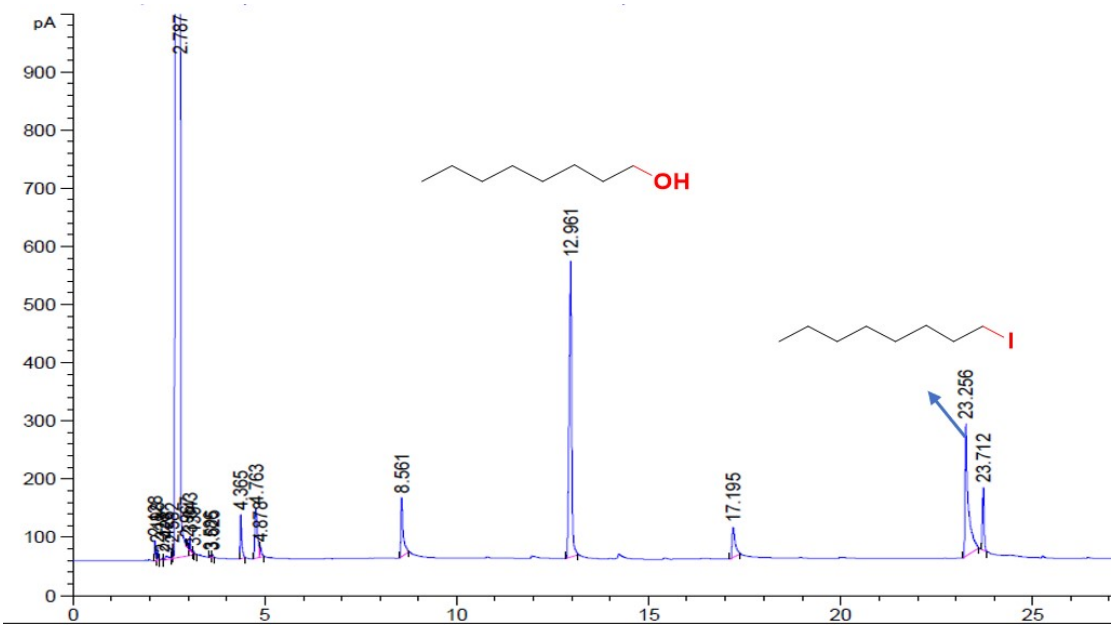


**Figure S56.** GC picture of 1-octanol disproportionation reaction product.

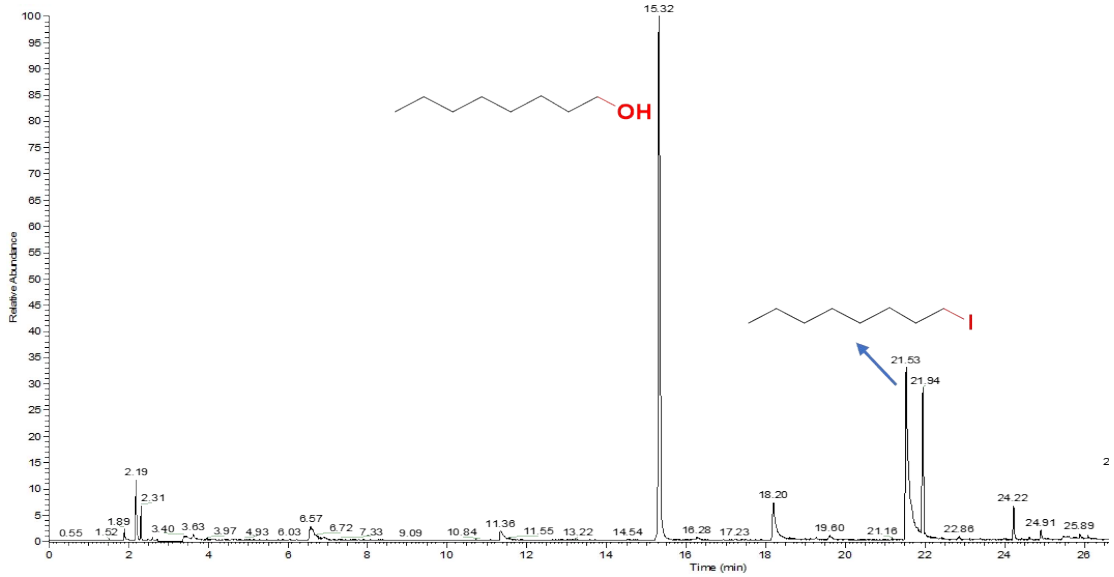


**Figure S57.** GCMS picture of 1-octanol disproportionation reaction product.

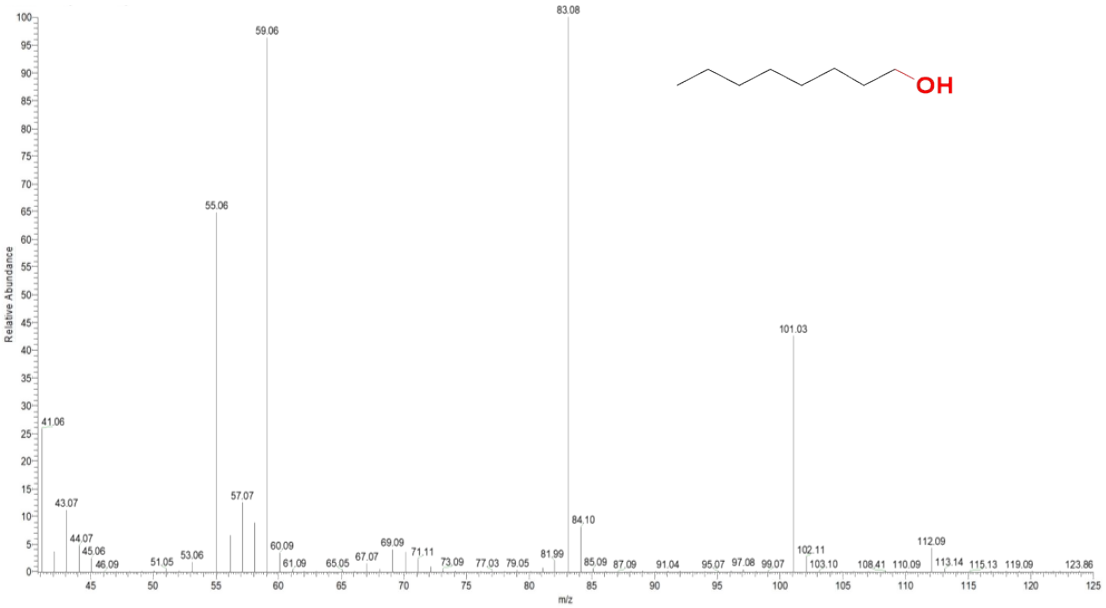


**Figure S58.** 1-octanol GCMS fragment peak graph.

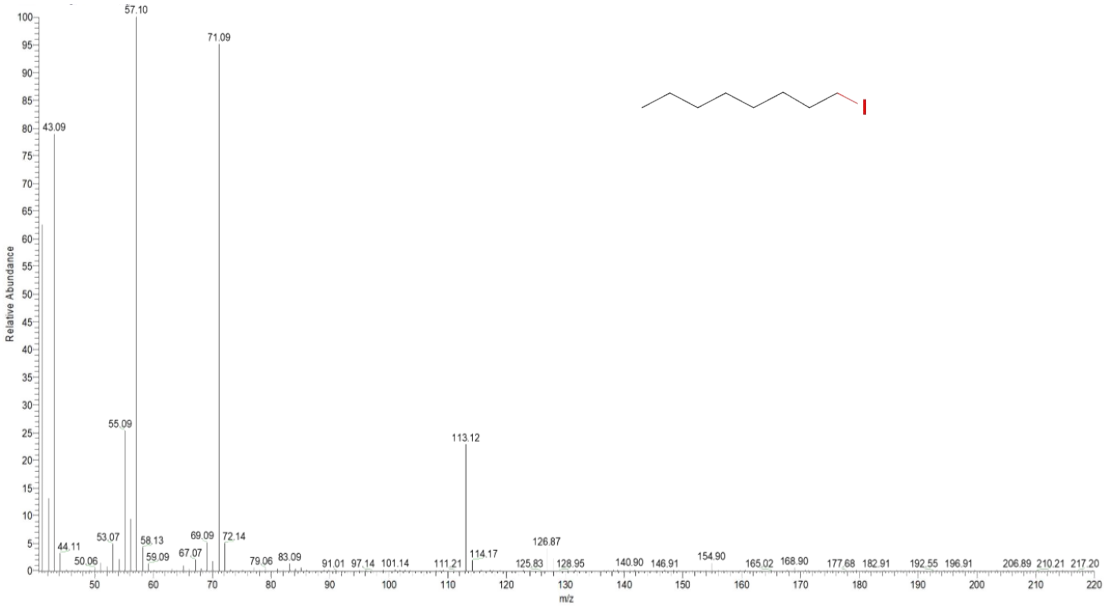


**Figure S59.** 1-octyliodide GCMS fragment peak graph.

## 9. Substrate range supplement

**Table S3** HI catalyzed disproportionation of allyl alcohol and benzyl alcohol.

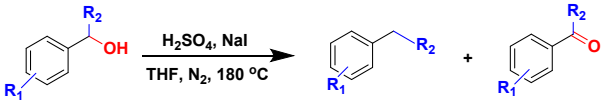


| Entry | Substrate | Conversion (%) | Product A | Selectivity A (%) | Product B | Selectivity B (%) |
|---|---|---|---|---|---|---|
| 1 | 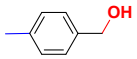 | >99 | 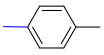 | 54 | 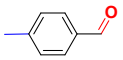 | 44 |
| 2 | 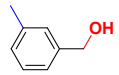 | >99 |  | 49 | 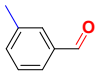 | 49 |
| 3 | 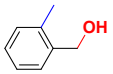 | >99 |  | 51 | 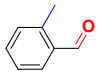 | 40 |
| 4 | 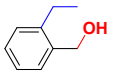 | >99 |  | 46 | 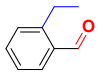 | 44 |
| 5 | 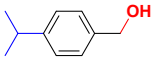 | >99 | 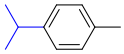 | 53 | 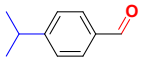 | 38 |
| 6 | 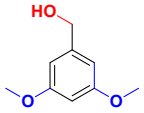 | >99 | 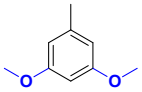 | 49 | 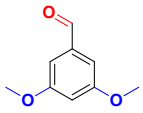 | 38 |
| 7 | 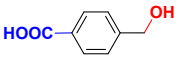 | >99 | 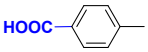 | 31 | 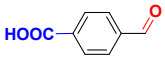 | 30 |
| 8 | 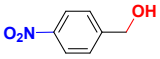 | 96 | 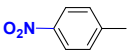 | 26 | 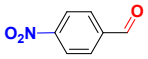 | 53 |

Reaction Condition: 1.0 mmol substrate, 0.6 mmol NaI, 0.3 mmol $H_2SO_4$, 6 mL THF, 500 rpm, 300 psi $N_2$, 180 ℃, 10 h. The above conversion and selectivity are determined by GC-MS and GC.

## 10. Bond dissociation energies databank

In the text table 3, the data was calculated using the website "iBonD - Nankai University." http://ibond.nankai.edu.cn/. Here is some detailed information about this website:

**iBonD 2.0 Version was Enriched!**

As known for its 1.0 version, the *i*BonD is a user-friendly internet-based databank of heterolytic ($pK_a$) and homolytic (BDE) bond dissociation energies, established by the bond energy team at Tsinghua University and Nankai University,

China. Now, it is upgraded to the 2.0 version. The most noteworthy features of *i*BonD 2.0 are: 1) 7500 homolytic bond dissociation enthalpy (BDE) values for over 5,000 representative organic compounds with various kinds of chemical bonds are now made readily searchable online, and 2) the p$K_a$ compilation is now substantially enriched to have more than 30,000 experimental equilibrium acidity data for about 20,000 compounds in various solvents. Thus, the *i*BonD 2.0 provides the heretofore most comprehensive bond energy collection and the most convenient approach to find the data with its powerful searching engine. Further updating of *i*BonD to compile the BDE values in solutions, the BDEs of metallic bonds, the energetics of some weak interactions (e. g. hydrogen bond, coordination bond) etc. will be done in our routine maintenances. The *i*BonD is provided free of charge for non-profit making academic use only. Whenever applicable, the users of the *i*BonD are requested to cite this website in their publication/presentation as following: **Internet Bond-energy Databank (p$K_a$ and BDE)--*i*BonD Home Page. http://ibond.chem.tsinghua.edu.cn** or **http://ibond.nankai.edu.cn**. All rights are reserved by the *i*BonD team.

## 11. Bond energy calculation

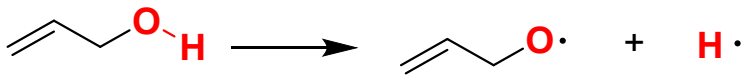


**Fig. S60.** The hydroxyl dissociation energy of allyl alcohol was not found in the database, so the following bond energy calculation was made.

1. Bond dissociation energy (BDE)

BDE = $\Delta_fH_{298}(CH_2{=}CH\text{-}CH_2O\cdot) + \Delta_fH_{298}(H\cdot) - \Delta_fH_{298}(CH_2{=}CH\text{-}CH_2OH)$

= (-192.442260) +(-0.499795) - (-193.098804)

= 0.156749 Ha

= 4.265 eV = 98.362 kcal/mol = 411.544 kJ/mol

2. Computing method

The DFT calculations were performed using Gaussian16[1] at the B3LYP [2]/ 6-

311G+(d,p) [3,4] level with the D3(BJ) empirical dispersion correction [5].

3. Source file description

The log file is a calculation output file, where Allyl alcohol.log corresponds to $CH_2$=CH-$CH_2$OH, Allyl alcohol free radical.log corresponds to $CH_2$=CH-$CH_2$O·, and Hydrogen radical.log corresponds to H·.

## 12. References


1. Gaussian 16, Revision A.03, M. J. Frisch, G. W. Trucks, H. B. Schlegel, G. E. Scuseria, M. A. Robb, J. R. Cheeseman, G. Scalmani, V. Barone, G. A. Petersson, H. Nakatsuji, X. Li, M. Caricato, A. V. Marenich, J. Bloino, B. G. Janesko, R. Gomperts, B. Mennucci, H. P. Hratchian, J. V. Ortiz, A. F. Izmaylov, J. L. Sonnenberg, D. Williams-Young, F. Ding, F. Lipparini, F. Egidi, J. Goings, B. Peng, A. Petrone, T. Henderson, D. Ranasinghe, V. G. Zakrzewski, J. Gao, N. Rega, G. Zheng, W. Liang, M. Hada, M. Ehara, K. Toyota, R. Fukuda, J. Hasegawa, M. Ishida, T. Nakajima, Y. Honda, O. Kitao, H. Nakai, T. Vreven, K. Throssell, J. A. Montgomery, Jr., J. E. Peralta, F. Ogliaro, M. J. Bearpark, J. J. Heyd, E. N. Brothers, K. N. Kudin, V. N. Staroverov, T. A. Keith, R. Kobayashi, J. Normand, K. Raghavachari, A. P. Rendell, J. C. Burant, S. S. Iyengar, J. Tomasi, M. Cossi, J. M. Millam, M. Klene, C. Adamo, R. Cammi, J. W. Ochterski, R. L. Martin, K. Morokuma, O. Farkas, J. B. Foresman, and D. J. Fox, Gaussian, Inc., Wallingford CT, 2016.
2. A. D. Becke, Density-Functional Thermochemistry. III. The Role of Exact Exchange. *J. Chem. Phys.*, 1993, **98**, 5648−5652.
3. W. J. Hehre, R. Ditchfield and J. A. Pople, Self-Consistent Molecular Orbital Methods. XII. Further Extensions of Gaussian-Type Basis Sets for Use in Molecular Orbital Studies of Organic Molecules. *J. Chem. Phys.*, 1972, **56**, 2257−2261.
4. P. C. Hariharan and J. A. Pople, The Influence of Polarization Functions on Molecular Orbital Hydrogenation Energies. *Theor. Chim. Acta*, 1973, **28**, 213−222.
5. S. Grimme, S. Ehrlich and L. Goerigk, Effect of the damping function in dispersion corrected density functional theory. *J. Comp. Chem.*, 2011, **32**, 1456-65.